PL-TR-94-2272

UV AND OPTICAL SPECTRA PRODUCED BY THE EXCEDE III EXPERIMENT

R.J. Rieder
T.J. Keneshea
A.J. LePage
S.A. Rappaport

Visidyne, Inc.
10 Corporate Place
South Bedford Street
Burlington, MA 01803

November 1994

Scientific Report No. 1

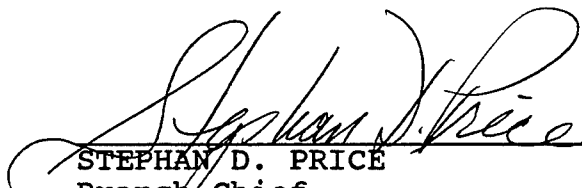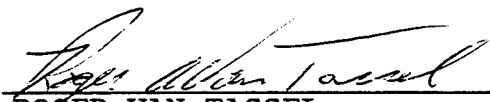Approved for Public Release; Distribution Unlimited

DTIC QUALITY INSPECTED ~

PHILLIPS LABORATORY
Directorate of Geophysics
AIR FORCE MATERIEL COMMAND
HANSCOM AIR FORCE BASE, MA 01731-3010

19970422 163

This technical report has been reviewed and is approved for publication

FRANCIS X. ROBERT
Contract Manager

STEPHAN D. PRICE
Branch Chief

ROGER VAN TASSEL
Division Director

REPORT DOCUMENTATION PAGE

Form Approved
OMB No. 0704-0188

1. AGENCY USE ONLY (Leave Blank)	2. REPORT DATE November 1994	3. REPORT TYPE AND DATES COVERED Scientific No. 1

4. TITLE AND SUBTITLE
UV and Optical Spectra Produced by the EXCEDE III Experiment

5. FUNDING NUMBERS
PE 63218C
PR S322 TA GG WU AE
Contr. F19628-93-C-0120

6. AUTHOR(S)
R.J. Rieder, T.J. Keneshea, A.J. LePage, and S.A. Rappaport

7. PERFORMING ORGANIZATION NAME(S) AND ADDRESS(ES)
Visidyne, Inc.
10 Corporate Place
South Bedford Street
Burlington, MA 01803

8. PERFORMING ORGANIZATION REPORT NUMBER

VI-2174

9. SPONSORING/MONITORING AGENCY NAME(S) AND ADDRESS(ES)
Phillips Laboratory
29 Randolph Road
Hanscom AFB, MA 01731-3010

Contract Manager: Frank Robert/GPOB

10. SPONSORING/MONITORING AGENCY REPORT NUMBER

PL-TR-94-2272

11. SUPPLEMENTARY NOTES

12a. DISTRIBUTION/AVAILABILITY STATEMENT

Approved for public release; distribution unlimited

12b. DISTRIBUTION CODE

13. ABSTRACT *(Maximum 200 words)*

A goal of the EXCEDE III (Excitation by Electron Deposition) atmospheric energy deposition experiment was to monitor the spectral excitations from the energy deposition profile produced by the ~ Ampere ~ 2.5 keV electron beam. During the EXCEDE III rocket flight on April 27, 1990, ultraviolet and optical spectra covering the wavelength region between 1800 and 800 Å were measured with two Ebert-Fastie spectrometers. Spectral features have been identified and line production efficiencies have been calculated. Finally, the measured spectra are compared with those obtained from natural aurora.

14. SUBJECT TERMS

EXCEDE III, Atmospheric Deposition, Artificial Aurora, UV Spectra, Optical Spectra

15. NUMBER OF PAGES
52

16. PRICE CODE

17. SECURITY CLASSIFICATION OF REPORT Unclassified	18. SECURITY CLASSIFICATION OF THIS PAGE Unclassified	19. SECURITY CLASSIFICATION OF ABSTRACT Unclassified	20. LIMITATION OF ABSTRACT SAR

Table of Contents

List of Figures

List of Tables

List of Plates

1. Introduction

EXCEDE III (*Ex*citation by *E*lectron *De*position) is an atmospheric energy deposition sounding rocket experiment that was launched on 27 April 1990 from White Sands Missile Range. The sounding rocket was configured as a separable payload. The "mother" payload module contained an electron accelerator and associated instrumentation while the "daughter" module contained the majority of sensors. Included as part of the EXCEDE III daughter payload were two Ebert-Fastie spectrometers and corresponding boresighted photometers operating at 3914 Å. A boresighted photometer was mounted on each spectrometer and was designed to have an identical field of view to that of the spectrometer. The two spectrometers scanned the spectral regions between 1800 and 3300 Å and 3000 and 8000 Å, respectively. The purpose of these instruments was to obtain profiles of the radiative processes of the excited atmosphere in the UV and visible region at a fixed angular distance along the beam from the accelerator module.

The configuration of the experiment and instrument complement have been described by *Rappaport et al.* [1993]. A schematic of the EXCEDE III flight configuration depicting the field-of-view of the spectrometers and the overall flight profile is shown in Figure 1. Each respective FOV is a slit that was oriented across the beam and was designed to be significantly wider than the beam diameter.

EXCEDE III is the fourth artificial aurora/atmospheric fluorescence sounding rocket experiment in a series that began in 1974. The first flight, PRECEDE, was launched at White Sands Missile Range on October 17, 1974 carrying a 2.5 kV, 0.8 A electron accelerator [*O'Neil et al.*, 1978a]. An electron beam was emitted beginning at 95 km on the upleg of the trajectory and through apogee at 120 km and down to 80 km on the downleg. During the second flight, EXCEDE II Test, the vehicle was spun at 1.9 Hz and deposited electrons in all directions as it rotated. The electron accelerators provided up to 10 A of current at 3 kV in the altitude range of 106 to 135 km [*O'Neil et al.*, 1978a]. Neither of these flights carried optical spectrometers.

EXCEDE SPECTRAL, flown on 18 October, 1979, injected 7 A of 3 keV electrons at altitudes similar to those in the previous two flights [*O'Neil et al.*, 1978b; *Lee et al.*, 1985] and
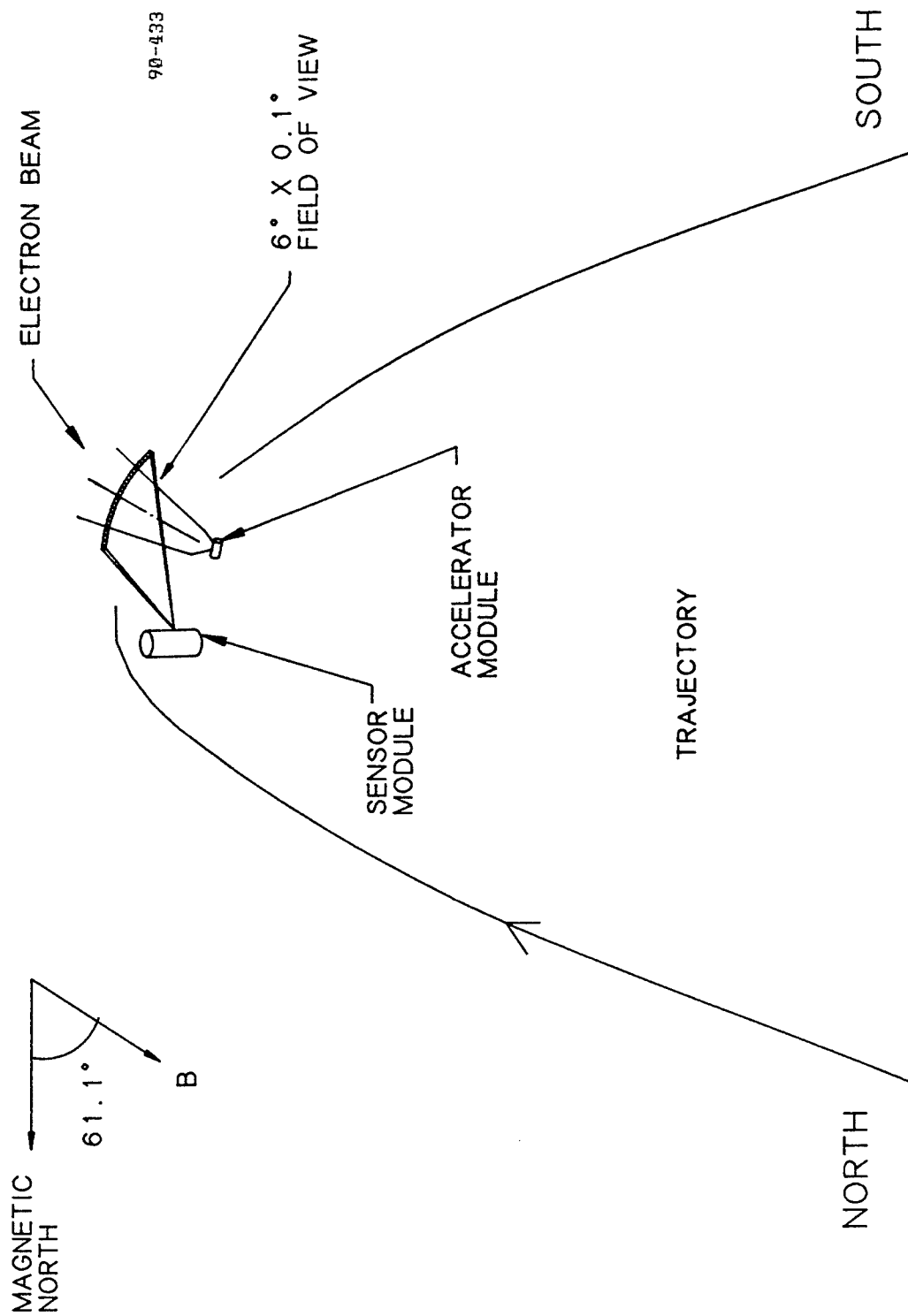
Figure 1: EXCEDE III Flight Configuration Showing Typical Spectrometer Field-of-View.

was the first experiment in this series to measure UV and visible spectra. It carried two Ebert-Fastie spectrometers on board with spectral ranges similar to those flown on the EXCEDE III payload. The EXCEDE SPECTRAL spectrometers did not contain any foreoptics, had FOVs of 12° × 12°, and had no corresponding boresight photometers for normalization. The electron accelerator and sensors both operated from the same platform, and as a result of their proximity, acquired spectra that were contaminated by outgassed water vapor from the skin of the sounding rocket.

The mother-daughter configuration used for the EXCEDE III flight successfully avoided any spectral contamination caused by outgassing. The EXCEDE III sounding rocket experiment also is distinguished from the earlier experiments by having emitted the largest amount of power ($\sim$ 45 kW) into the atmosphere.

2. Equipment

Two Ebert-Fastie spectrometers were included in the daughter payload and measured the optical signatures from electron impact excited regions of the atmosphere. The UV spectrometer scanned the spectral region from 1300 to 3300 Å although the spectral response was cut off at 1800 Å because of inadequate purging of O_2 in the payload; the visible spectrometer scanned the region between 3000 and 8000 Å. Both spectrometers contained additional foreoptics to reduce the fields-of-view to a long slit in order to make measurements of a thin slice of the beam at a fixed angular distance from the accelerator. This field-of-view was duplicated by an associated 3914 Å boresighted photometer and used to provide normalization of the beam intensity.

Figure 2 shows a schematic drawing of the spectrometers. Both spectrometers were made by Research Instruments Inc. (RSI) of Cockeysville, Md. (Model 16-251). Light incident on the entrance slit was reflected from a spherical mirror having a 1/4 meter focal length and focused onto a flat grating that rotated. The dispersed light was reflected back onto the spherical mirror and out the exit slit where it was detected with a photomultiplier tube.

The dynamic range of the instrument was expanded by a factor of $\sim$ 100 by periodically placing a neutral density filter in front of the entrance slit. During the flight the ND filter was

Figure 2: Schematic of a Ebert-Fastie Spectrometer.

ENTRANCE SLIT

N.D. 2.0 (typ.) COATING

UNCOATED

ALTERNATE SCAN ATTENUATOR DISC

CALIBRATION SOURCE

OPTICAL BAFFLE

12°

HERMETIC SEAL WINDOW

ENTRANCE SLIT

DETECTOR

GRATING

EXIT SLIT

1REV/2 SPECTRAL SCANS
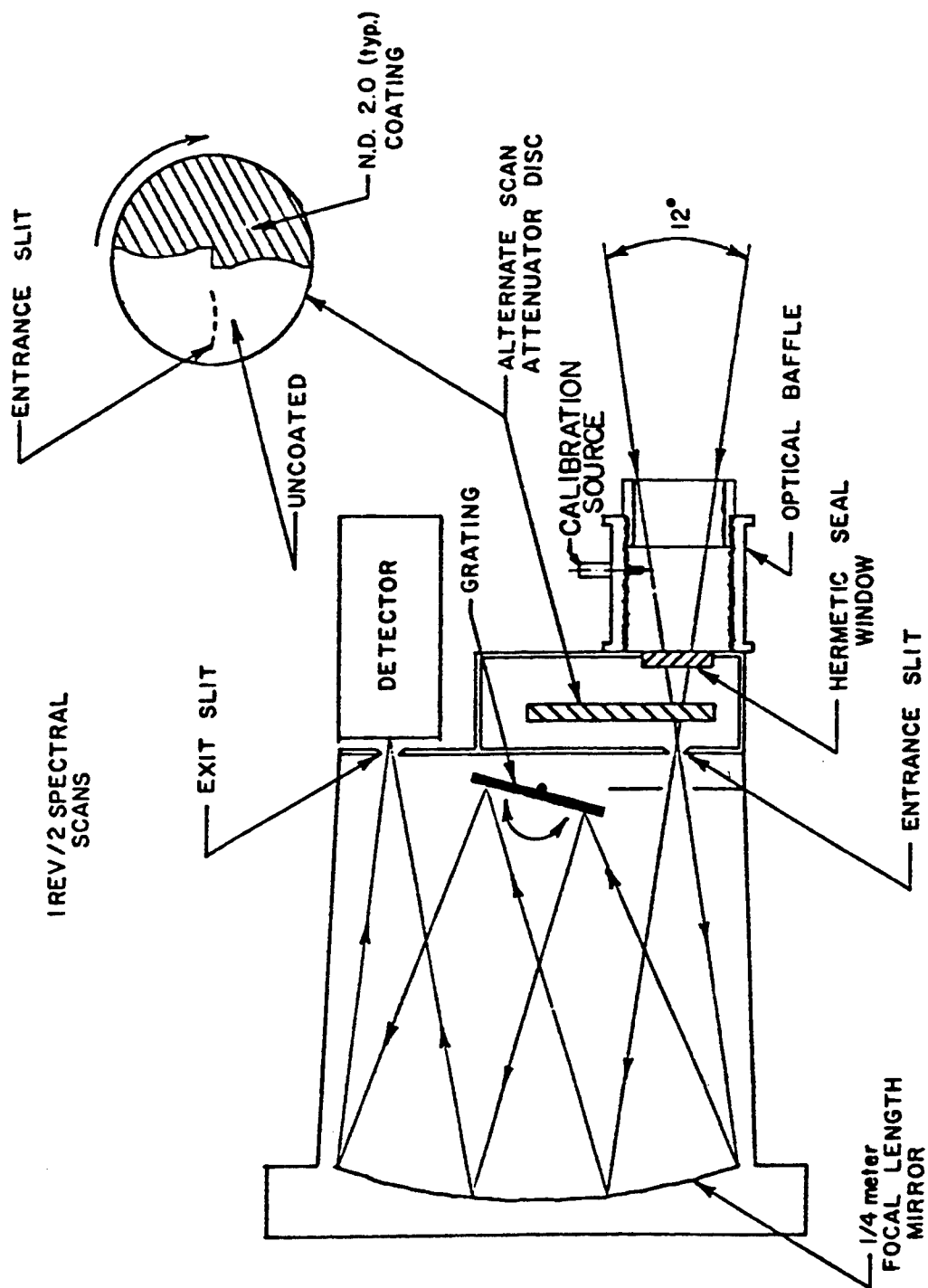
1/4 meter FOCAL LENGTH MIRROR

rotated into position during every other scan of the spectrometer. The filter wheel holding the neutral density glass also held order sorting filters designed to block the wavelengths caused by higher order dispersions.

The Ebert-Fastie spectrometer design was chosen because of its compactness, simplicity, stability, and spectral resolution [*Fastie*, 1952a; *Fastie*, 1952b; *Samson*, 1967]. This design was originally invented by *Ebert* [1889], and was rediscovered by Fastie who was responsible for additional refinements. A significant refinement was the use of curved slits at the entrance and exit apertures which resulted in the removal of astigmatism and better spectral resolution when long slits are used.

Table 1 is a list of characteristics of the UV and Visible Spectrometers.

Table 1: Specifications for UV and Visible Ebert-Fastie Spectrometers

Type:	UV	Visible
Focal Length:	1/4 Meter	1/4 Meter
Wavelength Range:	1300 to 3300 Å	3000 to 8000 Å
Spectral Resolution:	6 Å (FWHM)	13.2 Å (FWHM)
Slit Width:	0.036 cm	0.035 cm
Slit Length:	2.86 cm	2.54 cm
Field of View (incl. foreoptics)	~0.075° × 6°	~0.083° × 6°
AΩ:	4.45 × 10^{-3} cm^2-sr	3.85 × 10^{-3} cm^2-sr
Grating:	2400 l/mm blazed at 2400 Å; Al and Al/MgF$_2$ coating	1200 l/mm blazed at 5000 Å; Al and SiO$_2$ coating
Spectral Scan Rate:	2.1 Seconds	2.6 Seconds
Data Sampling Rate:	750 Samples/Seconds	750 Samples/Seconds

3. Post-Flight Calibration

Post-flight calibrations were performed on the spectrometers and boresighted photometers. Specifically, the wavelength calibrations for the two spectrometers used in the analysis were

reworked using in-flight data and more detailed measurements of the nonlinearity of the photomultiplier tubes were made.

3.1 *Wavelength Calibration.* The wavelength calibrations for the spectrometers were obtained using in-flight data. Previously, the wavelength was calibrated against the output of the an incremental encoder that registered the position of the spectral grating. This encoder was mechanically attached to the rotating axis of the spectral grating via a timing chain. It was determined that much better accuracy could be obtained if the sample number in the spectrum was used as an index in place of the encoder value. The improved accuracy is the result of better mechanical rigidity, however, jitter in the position of the grating of typically one sample is still evidenced (e.g. Plate 4).

The encoder information was used to determine the start of the a spectral scan. However, for mechanical reasons the start can be determined only to within a few samples and each scan must be registered to an arbitrary reference scan. This was done by choosing several well defined spectral features in each scan and adjusting the start of the scan until the wavelengths of the spectral features were in agreement with those of the reference scan.

3.2 *Nonlinearity.* The nonlinearity of the photomultiplier (PMT) counts as a function of incident photons was remeasured for the two photometers and the UV spectrometer. Unfortunately, the visible spectrometer was not able to be remeasured due to a failure of the PMT. The new measurements resulted in more data points on the non-linearity curve at high count rates and hence a better mapping of the region just before saturation occurs.

4. Boresight Photometers

A boresighted photometer measuring the $N_2^+(1N)$ 0-0 band at 3914 Å [*Rieder et al.*, 1993] was part of each spectrometer package and was designed to provide normalization against changes in the beam intensity for the spectral scans. Each photometer was mounted on the same

platform as its respective spectrometer and was designed with overlapping fields-of-view. Both photometers used narrow band filters centered at 3914 Å, each having a width of 14.4 $\pm$ 1 Å (FWHM).

The fields-of-view for each instrument are (2.72 $\pm$ 0.22) $\times$ 10^{-3} cm^2-sr and (1.89 $\pm$ 0.3) $\times$ 10^{-3} cm^2-sr for the UV and Visible photometers, respectively. A mapping of the field-of-view for the UV boresight photometer is shown in Figure 3. This FOV is characteristic of those seen for the UV and Visible spectrometers and the other boresight photometer. The ridge crest has been smoothed to remove spurious spikes introduced from the computer graphics interpolation scheme.

The calibration was applied to the two data sets and their respective intensities are shown in Figures 4a and 4b as a function of time. The two plots are in good agreement with each other and provide the temporal history of the beam. The data are presented here in a form that can be used to normalize the spectrometer. Because the field-of-views are the same for the photometer and its respective spectrometer, the two instruments are exposed to the same geometric efficiencies and may be divided into each other. The fields-of-view are long slits that are underfilled by the beam for most of the flight. The profiles shown in Figure 4 have *not* been corrected for this geometry and therefore cannot be treated as a measurement of the energy deposition per unit length of the beam.

The intensity profile for the 3914 Å emission follows the atmospheric density. The lowest intensities being at apogee where the density is smallest and increasing in intensity at lower altitudes. Other prominent features in the profile are two lower intensity pulses between 205 and 218 seconds. These two pulses have been confirmed by other independent measurements to result from a reduction in the accelerator output. Other artifacts such as electrical load faults from the electron accelerator (e.g. t = 151 seconds) and beam power oscillations caused by interference from the attitude control system [*Rieder et al.*, 1993] are also seen.

A running average over nine samples (12 ms) was applied to the data to reduce the fluctuations from counting statistics. In addition, data from both of the boresighted photometers become saturated at the lower altitudes and cannot be used to normalize their respective spectrometers. A comparison of these data with comparable data from the EXCEDE III X-ray experiment [*Rappaport et al.*, 1993], indicate that the X-ray data set can be used in place of the

7
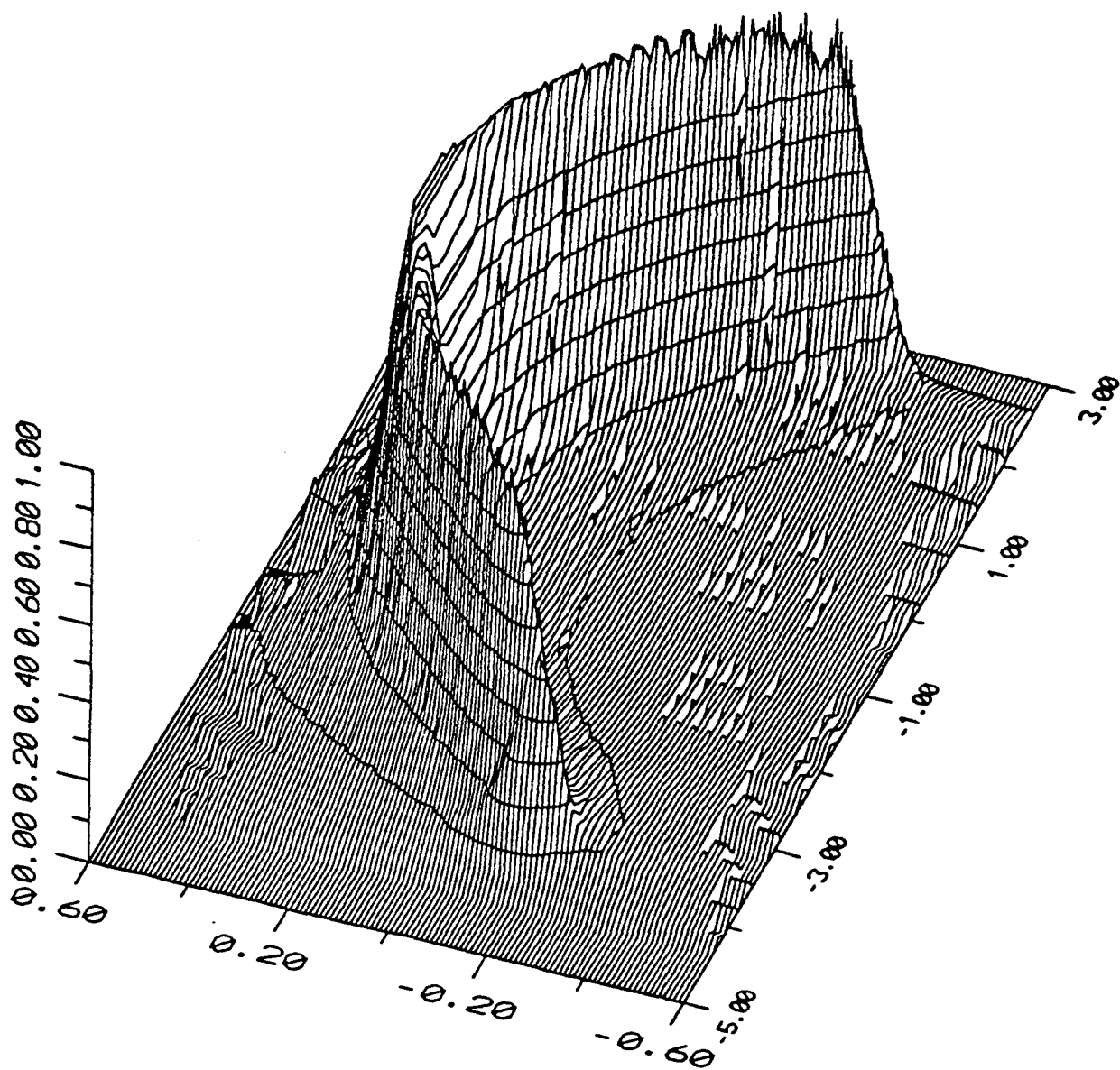
Figure 3: Measured Field-of-View From the UV Boresight 3914 Å Photometer.
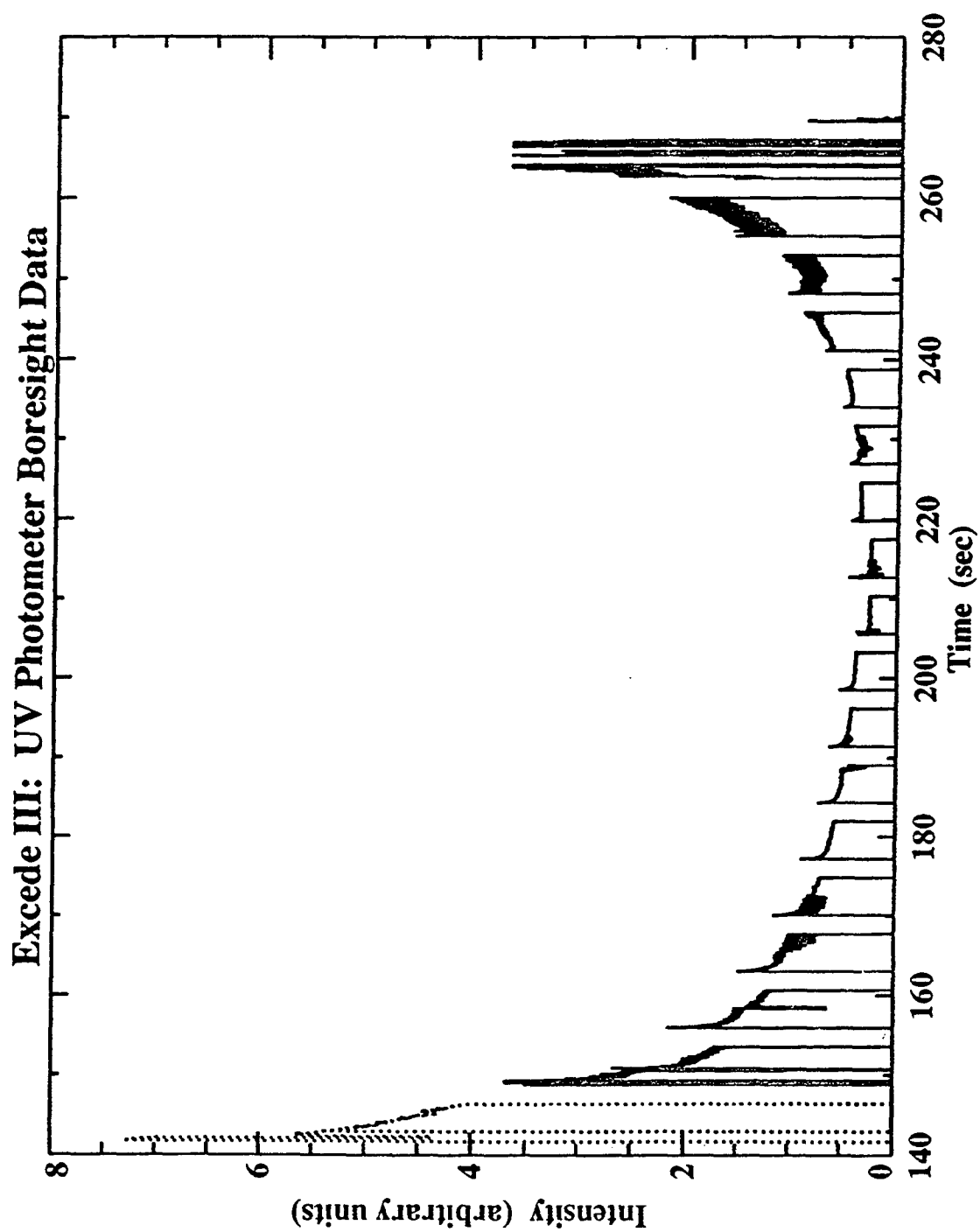
Excede III: UV Photometer Boresight Data

Figure 4a: Flight Profile of the UV Boresight 3914 Å Photometer.

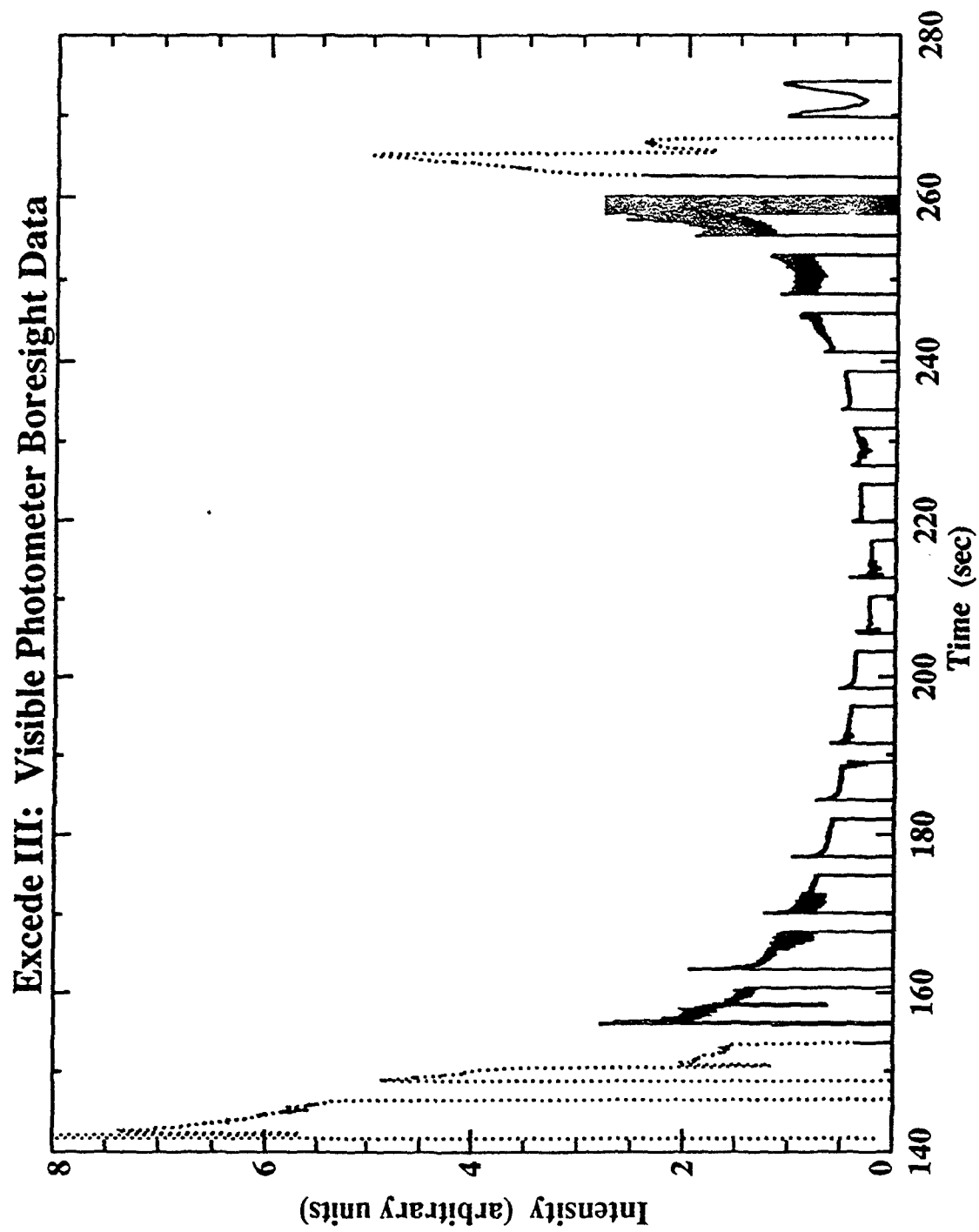9

Excede III: Visible Photometer Boresight Data

Figure 4b: Flight Profile of the Visible Boresight 3914 Å Photometer.

10

saturated optical data set for normalizing the beam intensity. The X-ray data have been scaled and substituted for the optical data when the latter is in saturation in order to reclaim the low-altitude spectral scans. The times when X-ray data are used are denoted in the figure by a dotted line. The UV boresight data set required substitution of X-rat data for only one pulse at 142 seconds (pulse 4 - maximum dose); these data were used to normalize UV spectral scan numbers 5, 6, and 7. The Visible boresight photometer utilizes X-ray data at 142, 149, and 262 seconds (beam pulses 4, 5, and 21); these data correspond to Visible spectrometer scan numbers 4 through 8 and 48 through 49.

5. Analysis and Results

5.1 *Presentation of Data.* The data are presented in several forms. Plates 1 and 2 are spectrograms of the entire UV and Visible data sets and are intended to provide an overview of the data to the reader. The wavelength and intensity (telemetry voltage to counting rate) calibrations have been applied to the data; however, background subtraction and normalization with respect to the beam intensity have not been performed.

Figures 7a and 7b are line plots showing typical spectral scans afer any backgrounds have been subtracted off and the spectra have been normalized with respect to the beam intensity using the boresight photometer data sets.

Plates 3 and 4 are spectrograms of the unattenuated spectral scans only and have been designed to provide a direct comparison of scans at different altitudes. These spectrograms have been constructed from line plots similar to those shown in Figures 7a and b. The background has been subtracted and the spectra have been normalized with respect to the beam intensit y as determined by the boresight photometers. Each spectral scan has been normalized to the N_2^+ (1N) 0-1 band at 4278 Å.

5.2 *UV Spectrometer.* A total of 27 scans contain usable data and, of those scans, 14 complete scans are available. Table 2 is a list of the time and corresponding altitude of the start of each scan along with the portion of the scan having spectral information. A visual display of this

11

EXCEDE III UV Spectral Scans
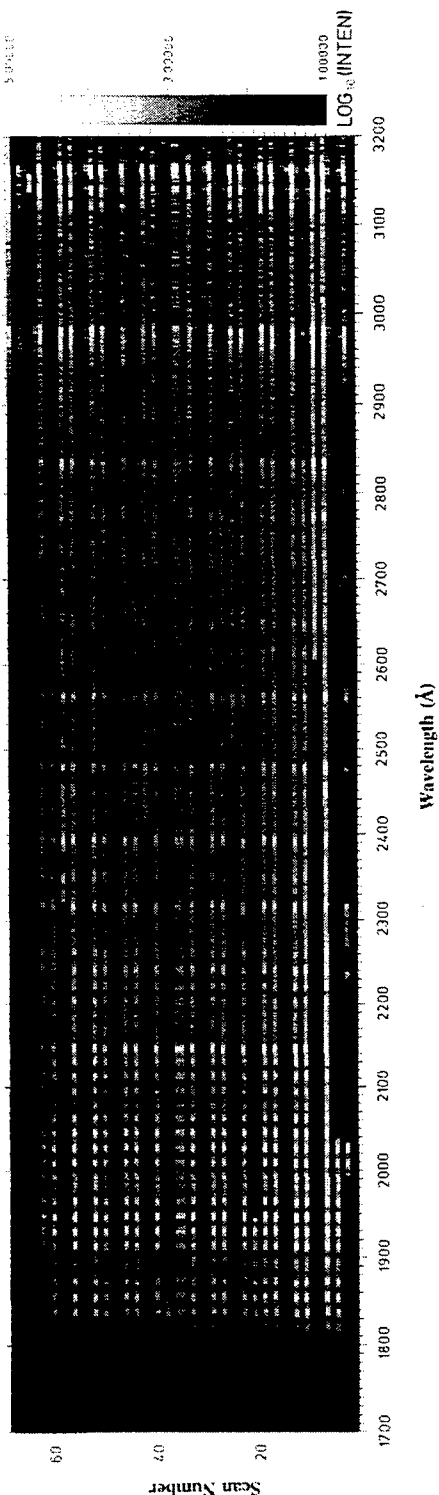
Plate 1: EXCEDE III UV spectral scans (1800-3300 Å).

EXCEDE III Visible Spectral Scans
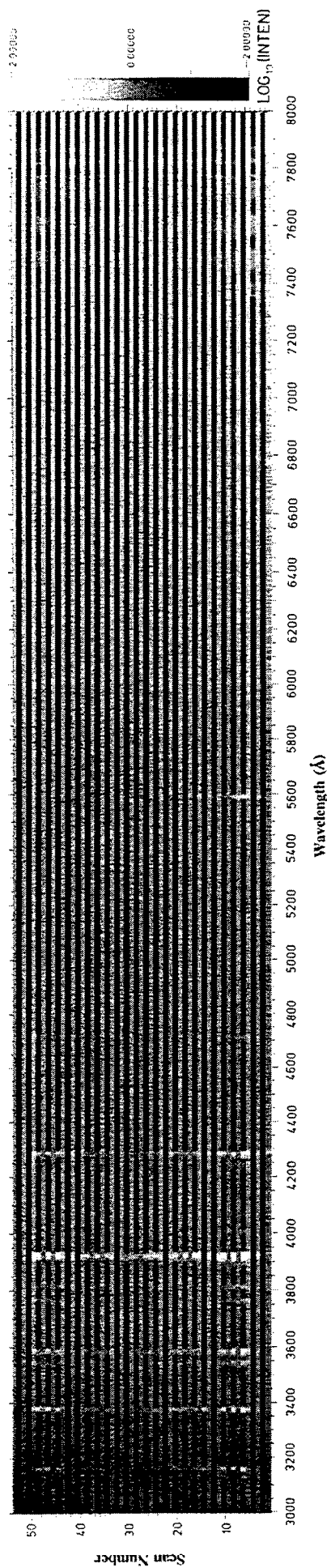
Plate 2: EXCEDE III visible spectral scans (3000-8000 Å).

12

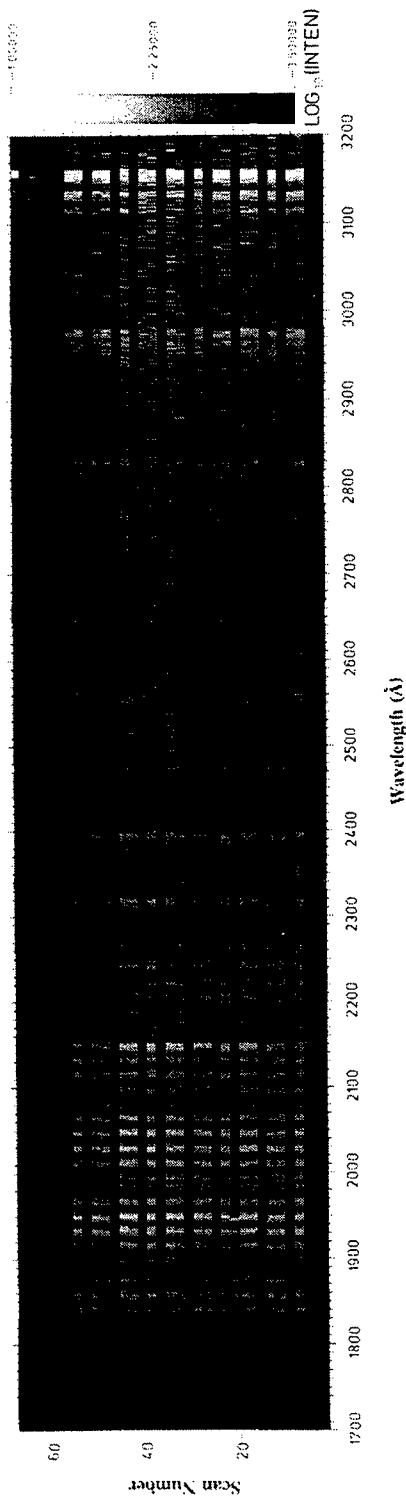## EXCEDE III Unattenuated UV Spectra

Plate 3: EXCEDE III unattenuated UV spectra (1800-3300 Å).
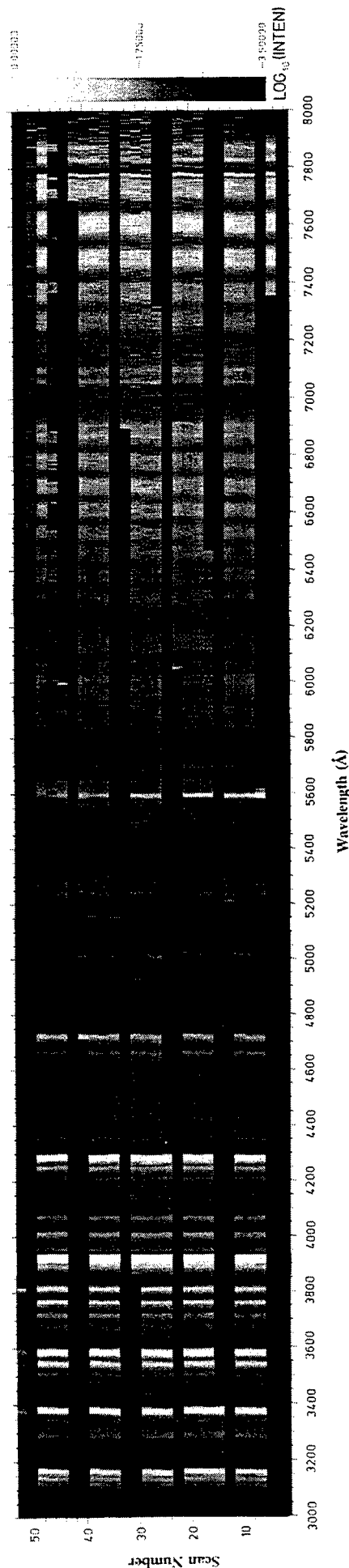
EXCEDE III Unattenuated Visible Spectra

Plate 4: EXCEDE III unattenuated visible spectra (3000-8000 Å).

N.B.: All spectral scans in Plates 3 and 4 have been normalized using their associated 3914 Å boresight photometers and have been referenced to the $N_2(2P)$ 0-1 emission at 4278 Å.

13

Table 2: EXCEDE III UV Spectrometer Scans

Scan No.	Start Time (sec)	Altitude (km)	Wavelength Range (A)	Scan No.	Start Time (sec)	Altitude (km)	Wavelength Range (A)
				35	208.576	114.128	-
1	132.935	96.772	-	36	210.798	113.819	1800 - 1840
2	135.160	98.056	2900 - 3200	37	213.024	113.463	-
3	137.386	99.293	-	38	215.248	113.060	1800 - 3200
4	139.610	100.482	-	39	217.472	112.610	-
5	141.834	101.624	-	40	219.698	112.114	2400 - 3200
6	144.059	102.721	1800 - 3200	41	221.921	111.570	-
7	146.283	103.769	1800 - 2470	42	224.146	110.980	1800 - 2680
8	148.507	104.771	3000 - 3200	43	226.372	110.343	-
9	150.731	105.727	-	44	228.598	109.659	1800 - 3200
10	152.956	106.635	1800 - 2850	45	230.821	108.928	-
11	155.182	107.498	-	46	233.045	108.151	-
12	157.407	108.313	1800 - 3200	47	235.269	107.327	-
13	159.631	109.081	-	48	237.494	106.455	1800 - 3200
14	161.856	109.802	-	49	239.719	105.537	-
15	164.082	110.477	-	50	241.944	104.572	1800 - 3200
16	166.306	111.104	1800 - 3200	51	244.168	103.560	-
17	168.528	111.684	-	52	246.393	102.501	-
18	170.752	112.218	1800 - 3200	53	248.619	101.395	-
19	172.978	112.705	-	54	250.843	100.243	1800 - 3200
20	175.203	113.145	1800 - 1950	55	253.068	99.044	-
21	177.428	113.539	-	56	255.293	97.798	2320 - 3200
22	179.654	113.886	1800 - 3200	57	257.518	96.505	-
23	181.877	114.185	-	58	259.742	95.166	1800 - 2590
24	184.104	114.438	2500 - 3200	59	262.071	93.713	-
25	186.328	114.644	-	60	264.191	92.346	1800 - 2200
26	188.552	114.803	1800 - 2760	61	266.416	90.865	-
27	190.776	114.916	-	62	268.641	89.338	-
28	193.001	114.981	1800 - 3200	63	270.865	87.764	-
29	195.225	115.000	-	64	273.092	86.142	-
30	197.449	114.972	-	65	275.316	84.475	-
31	199.674	114.897	-	66	277.540	82.761	2500 - 3200
32	201.900	114.775	1800 - 3200	67	279.764	81.000	-
33	204.125	114.606	-				
34	206.350	114.390	1800 - 3200				

information is shown in Figure 5. Each spectral scan is represented on the figure as a square. The darkened fraction of a square indicates the portion of the scan having spectral data.

The UV spectrometer data set for the entire flight is shown in Plate 1. The UV data set has been calibrated and is plotted as a function of wavelength. The scan number is plotted along the y-axis and is commensurate with the mission elapsed time.

No spectral information is seen below 1800 Å although the UV spectrometer was designed to operate down to wavelengths as short as 1300 Å. This unexpected spectral attenuation is likely due to inadequate purging of the payload and absorption of these shorter wavelengths by oxygen. We have calculated the amount of O_2 needed to attenuate the wavelength response at 1800 Å and find it is consistent with measurements of the pressure inside the payload during the flight.

The dark portions between scans represent times when the electron beam was turned off. The duty cycle of the beam was not synchronized with the spectrometer scan rate and consequently the beat frequency of the two periods is seen.

Every other scan contains very little signal implying that the signal strengths were not strong enough to operate within the dynamic range of the attenuated scans. Therefore, the spectral scans with the neutral density filter in place contain almost no useful information and only the unattenuated UV spectral scans provide significant spectral data.

A series of spectral emissions appear relatively close together below ~2200 Å. Other well defined spectral features are also observed and appear to get wider and spaced farther apart as longer wavelengths are approached. Relatively bright emissions are seen above ~2800 Å.

Scans with the beam turned off have been studied to examine background levels from the UV spectrometer. The corresponding signals are found to be negligible, therefore, no background corrections are required.

5.3 *Catalog*. The UV spectrometer data set has been cataloged and is presented in Appendix B. Page one of the appendix is a list of the time, altitude, and spectral range for each scan that was previously shown in Table 2. The odd numbered scans were obtained with the neutral

15

EXCEDE III - UV Spectrometer Scans

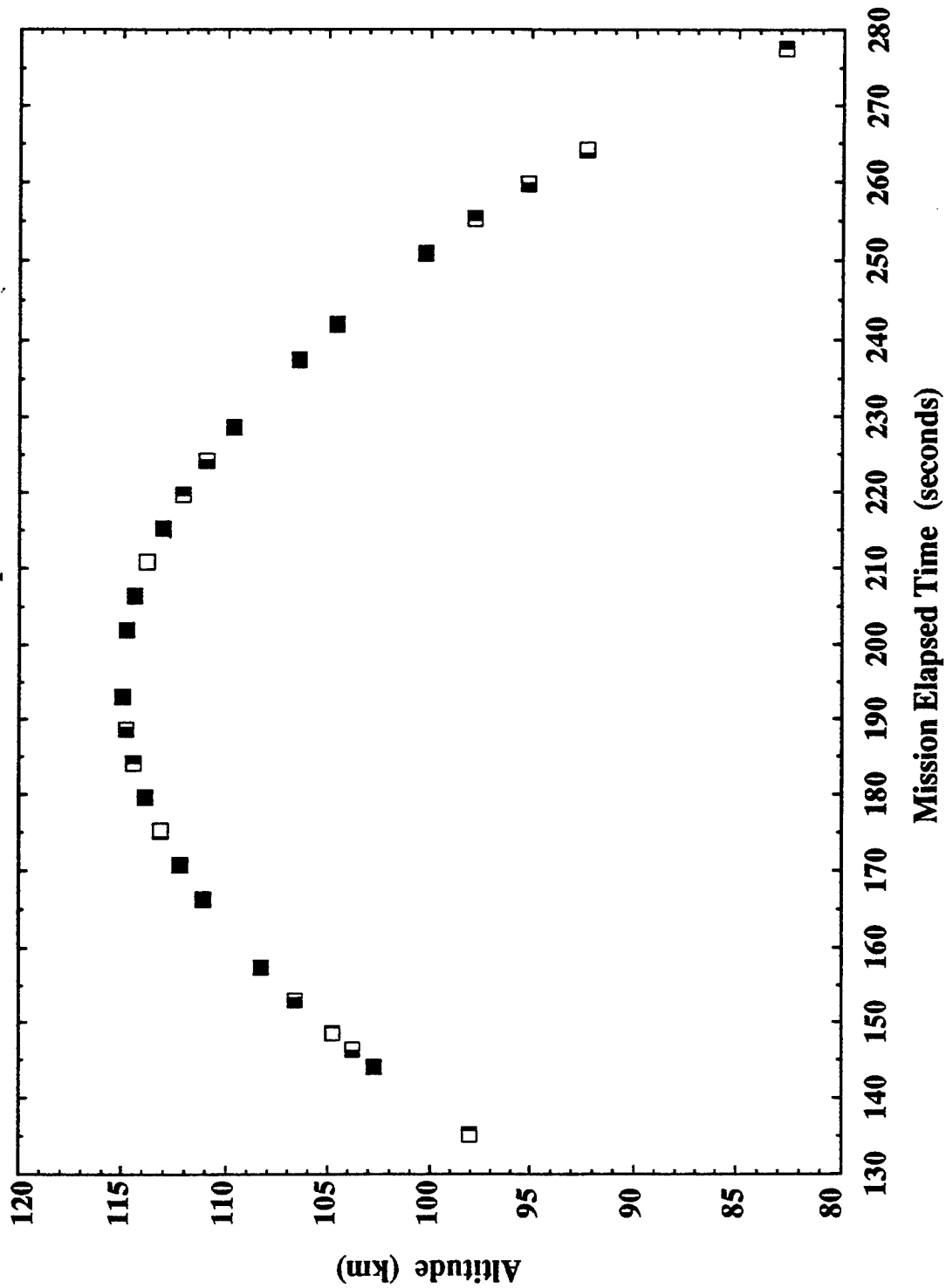Altitude (km)

Mission Elapsed Time (seconds)

Figure 5: UV Spectrometer Scan Times, Altitudes, and Length of Spectral Scan.

density filter in place. These attenuated scans contain no signal or background and while they are included in the list they have not been included in this catalog. Blank scans obtained with the beam turned off were also not included.

All scans appearing in the appendix have been normalized to the UV boresight photometer data set and are plotted with a linear intensity scale. Each UV spectral scan has been normalized to the nearest visible spectral scan using the $N_2(2P)$ 1-0 emission at 3159 Å which both scans have in common. This ultimately relates the UV spectrum to the $N_2^+(1N)$ 0-1 band at 4278 Å, where the band intensity has been defined to be equal to one.

5.4 *Visible Spectrometer.* The Visible spectrometer data set contains a total of 53 scans, and of those scans 10 complete unattenuated scans are available. Table 3 is a list of the start times of usable scans, the altitudes at the start of these scans, and their respective wavelength ranges. A graphic display of this spectral scan information is presented in Figure 6. The darkened fraction of each square represents the portion of the spectral scan containing useful data.

The Visible spectrometer was used to make measurements between 3000 and 8000 Å which overlap with the UV spectral data over the range 3000 to 3300 Å. The Visible spectrometer data set for the entire flight is shown in Plate 2. The calibration has been applied to the raw data and these data are plotted against their respective wavelengths. The scan number is plotted along the y-axis and is proportional to the mission elapsed time. Again the darkest portions of the scans represent times when the electron beam was turned off. The beam cycle period was not synchronized with the spectrometer scan cycle and consequently there is a beat frequency between the two periods. Half of the scans have been attenuated with a neutral density filter; these scans appear as the gray areas sandwiched between the blue (higher intensity) strips.

Several bright well defined emissions are seen between 3150 and 4700 Å. The most prominent emission is the 3914 Å band that is also identified as a prominent emission feature in natural aurora. The 5577 Å emission from atomic oxygen is also easily identified in this plate. The spectrogram shows an overall enhancement in intensity at wavelengths greater than ~6000 Å; this is primarily due to the $N_2(1P)$ series in conjunction with an increasing

17

Table 3: EXCEDE III Visible Spectrometer Scans

| Scan No.	Start Time (sec)	Altitude (km)	Wavelength Range (A)	Scan No.	Start Time (sec)	Altitude (km)	Wavelength Range (A)
				28	207.760	114.230	3000 - 8000
1	132.212	96.345	-	29	210.558	113.855	3000 - 4700
2	135.010	97.470	-	30	213.357	113.405	3800 - 8000
3	137.808	99.522	3500 - 6800	31	216.154	112.882	3000 - 7800
4	140.606	100.999	-	32	218.952	112.285	6850 - 8000
5	143.403	102.402	3000 - 8000	33	221.750	111.614	3000 - 8000
6	146.202	103.732	3000 - 5600	34	224.548	110.869	3000 - 5150
7	149.000	104.987	4700 - 8000	35	227.345	110.049	4300 - 8000
8	151.798	106.168	3000 - 8000	36	230.144	109.156	3000 - 8000
9	154.598	107.276	-	37	232.941	108.188	-
10	157.395	108.308	3000 - 8000	38	235.740	107.146	3000 - 8000
11	160.194	109.267	3000 - 6000	39	238.538	106.030	3000 - 5600
12	162.991	110.152	5180 - 8000	40	241.336	104.840	4700 - 8000
13	165.788	110.962	3000 - 8000	41	244.130	103.576	3000 - 8000
14	168.587	111.699	3000 - 3500	42	246.932	102.238	7680 - 8000
15	171.384	112.361	3000 - 8000	43	249.730	100.826	3000 - 8000
16	174.183	112.949	3000 - 6500	44	252.527	99.340	3000 - 6100
17	176.980	113.464	5600 - 8000	45	255.324	97.780	5100 - 8000
18	179.779	113.904	3000 - 8000	46	258.123	96.145	3000 - 8000
19	182.578	114.270	3000 - 3900	47	260.920	94.437	-
20	185.377	114.562	3000 - 8000	48	263.719	92.654	3000 - 8000
21	188.174	114.780	3000 - 6900	49	266.516	90.798	3000 - 6400
22	190.972	114.923	6000 - 8000	50	269.315	88.866	6050 - 8000
23	193.770	114.993	3000 - 8000	51	272.114	86.861	3000 - 8000
24	196.568	114.988	3000 - 4300	52	274.911	84.782	3000 - 3800
25	199.365	114.910	3500 - 8000	53	277.708	82.630	3500 - 8000
26	202.164	114.757	3000 - 7300				
27	204.961	114.530	6400 - 8000				
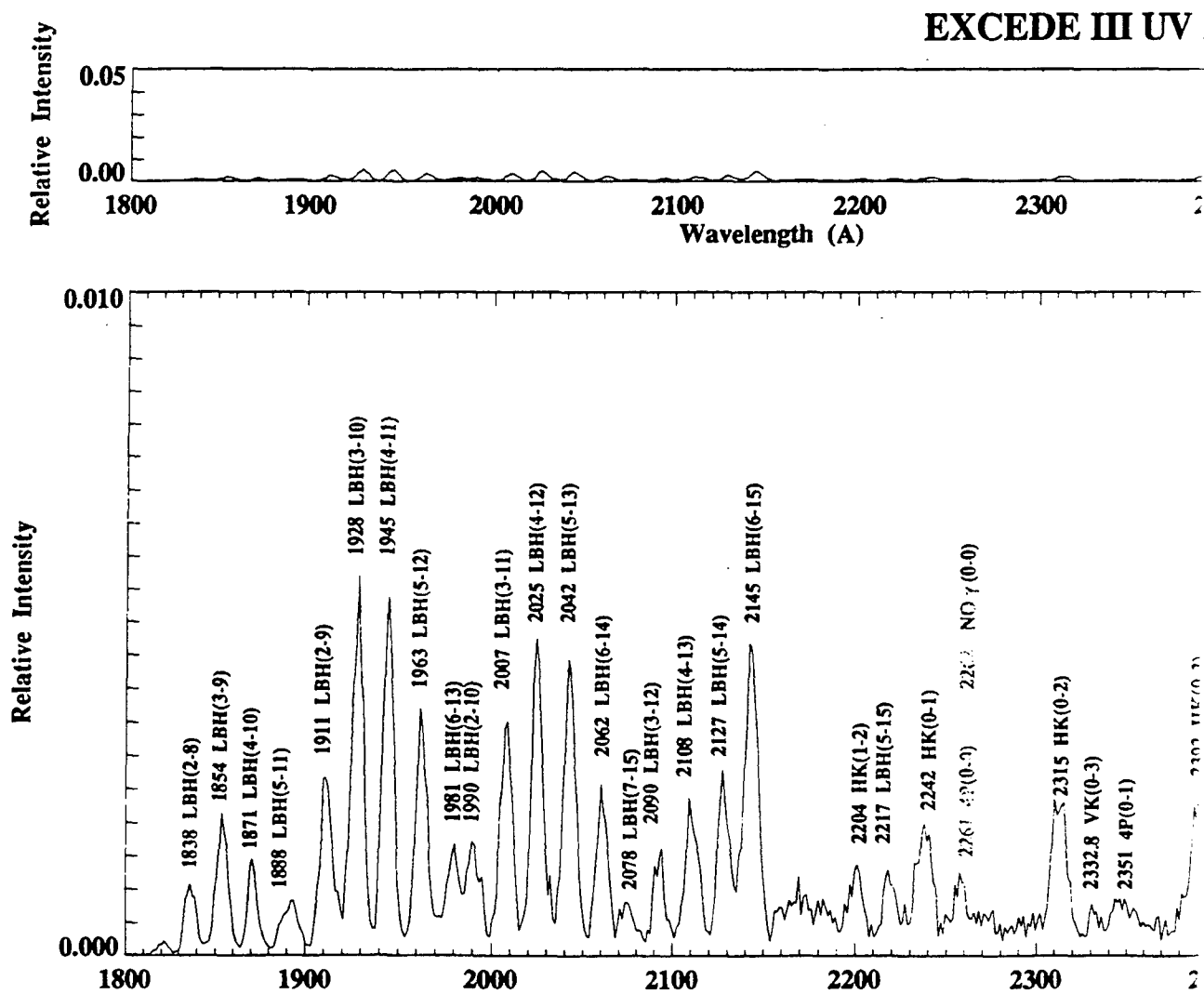
Figure 7a: UV Spectr

EXCEDE III UV SCAN No. 12 at 157.4 Sec. and 108.3 Km.
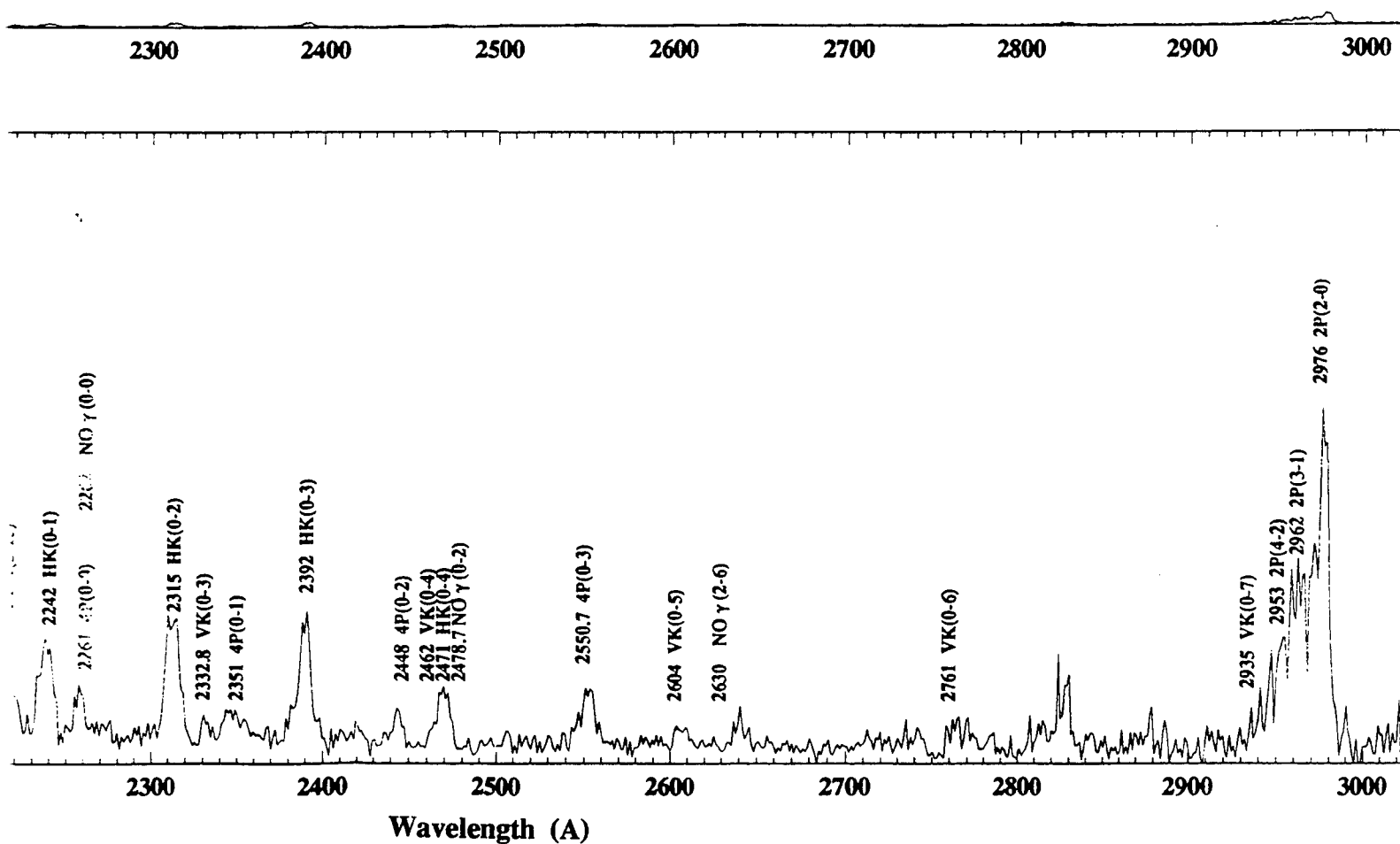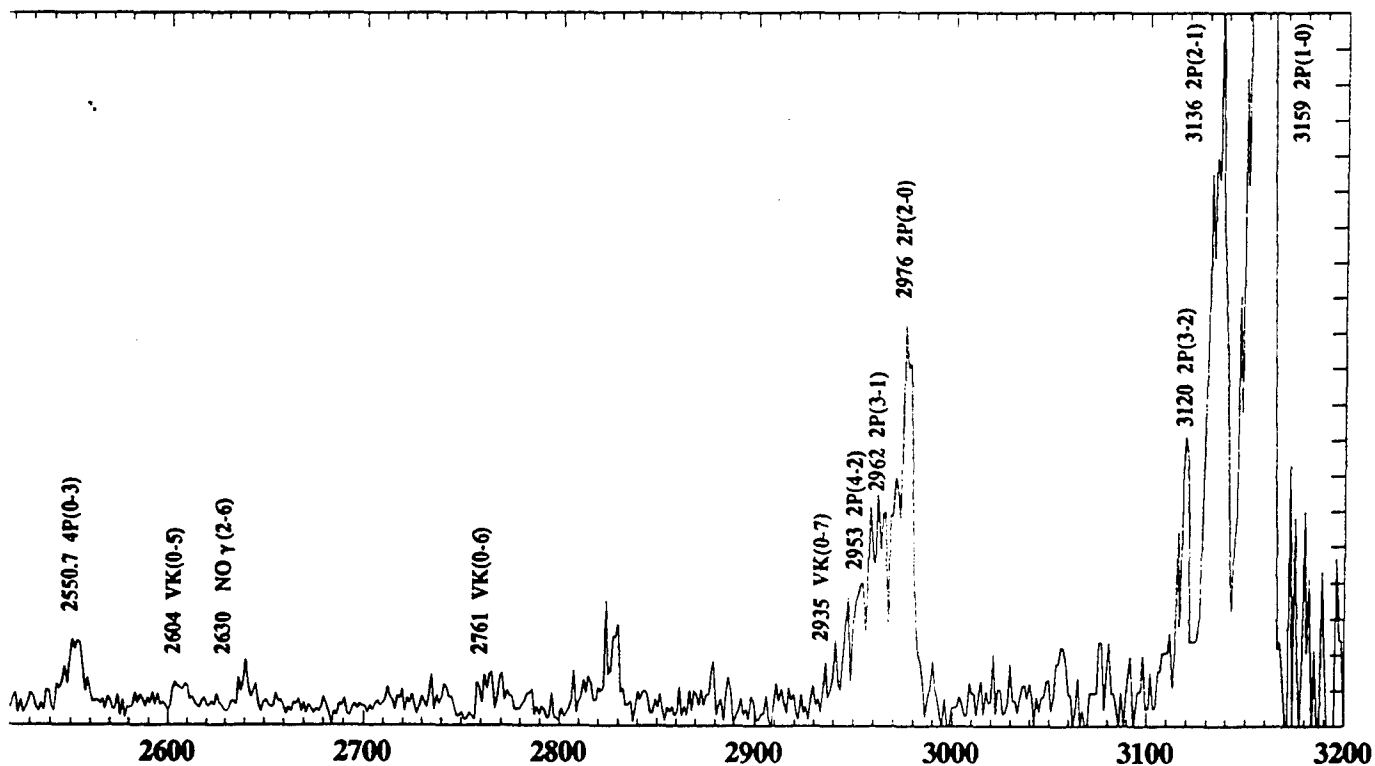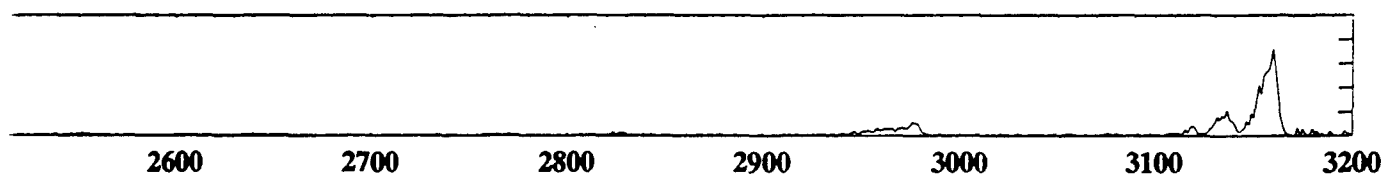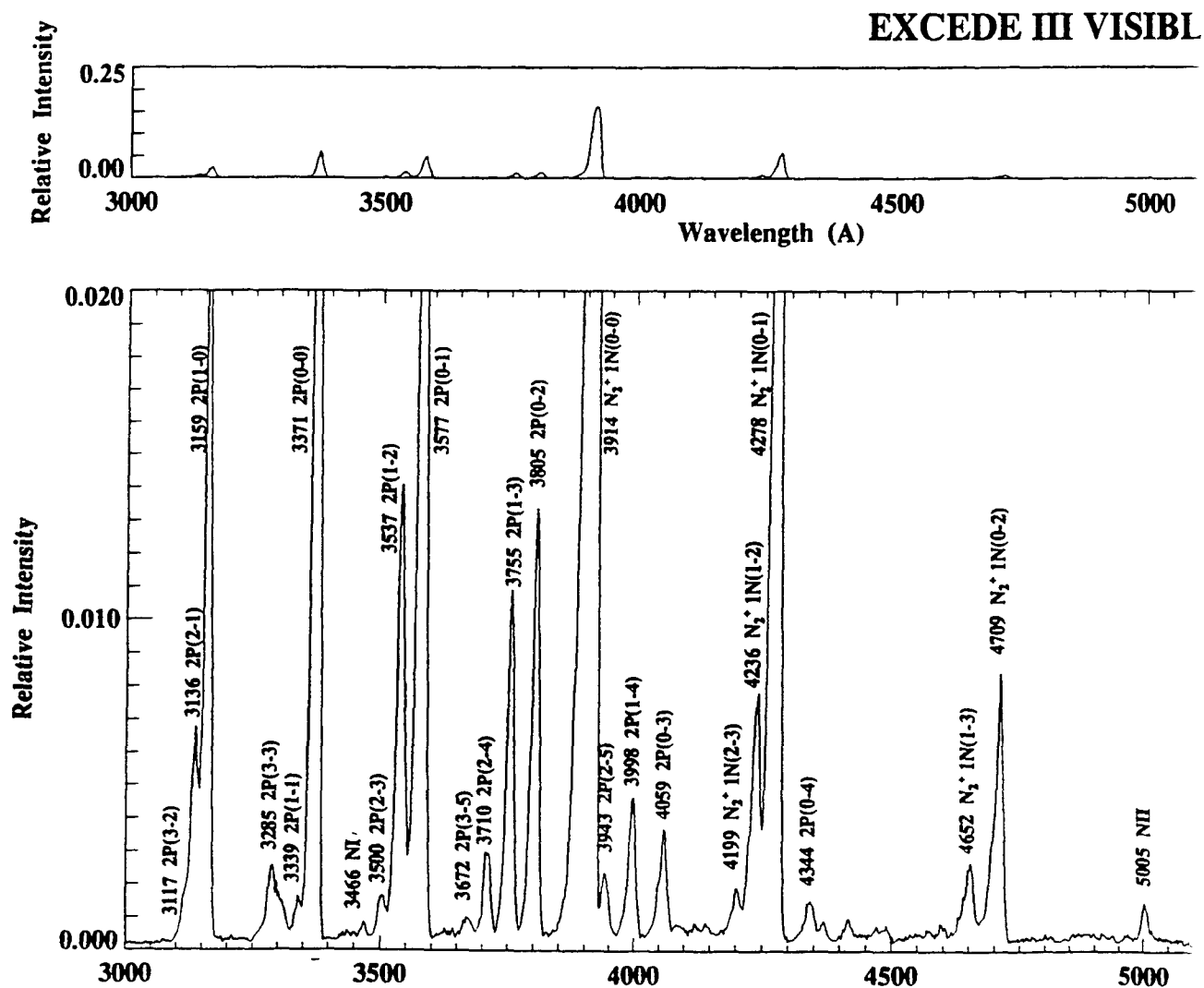

Figure 7a: UV Spectrum at 108.3 km From the EXCEDE III Experiment.

(A)

from the EXCEDE III Experiment.

③

Figure 7b: Optical Sp

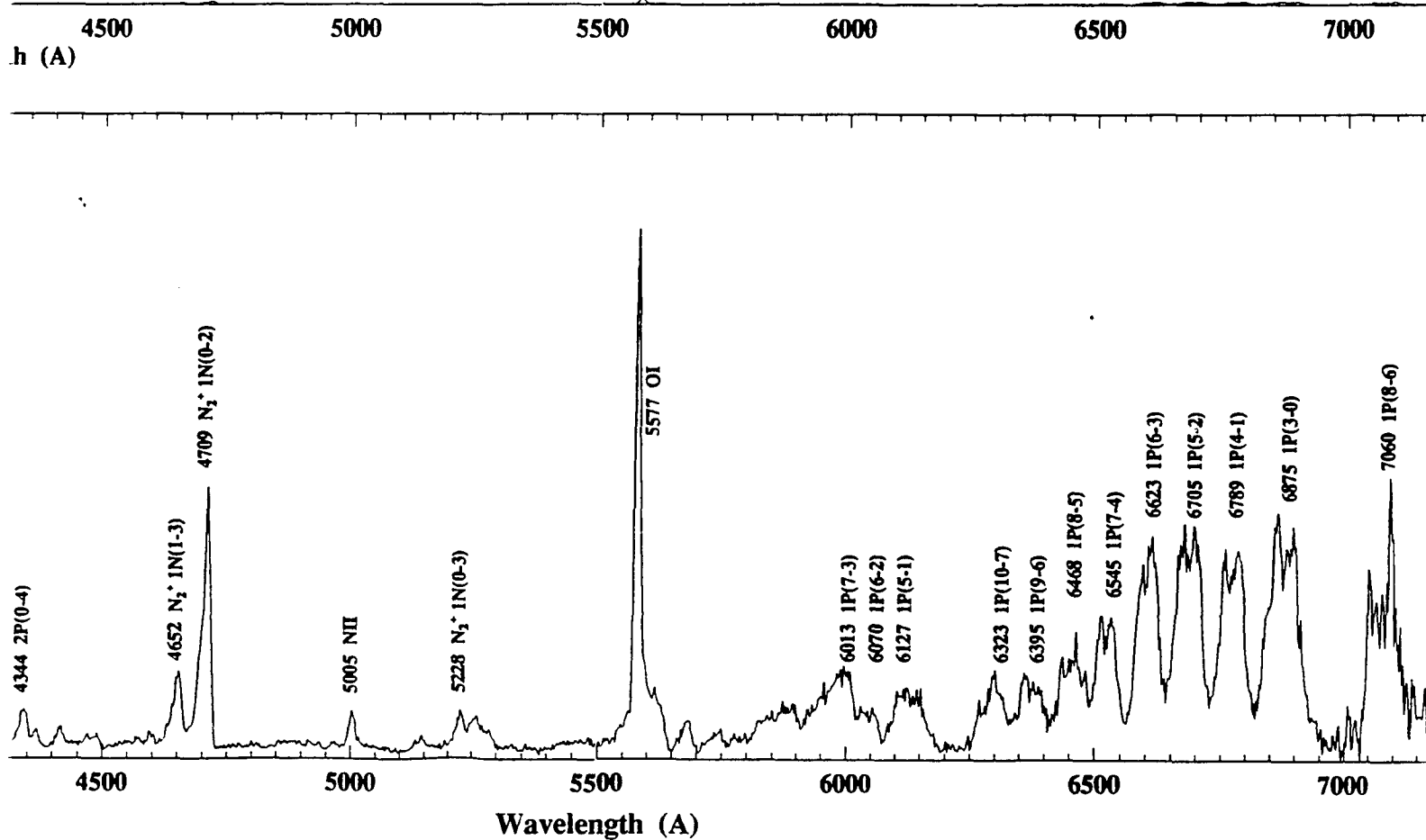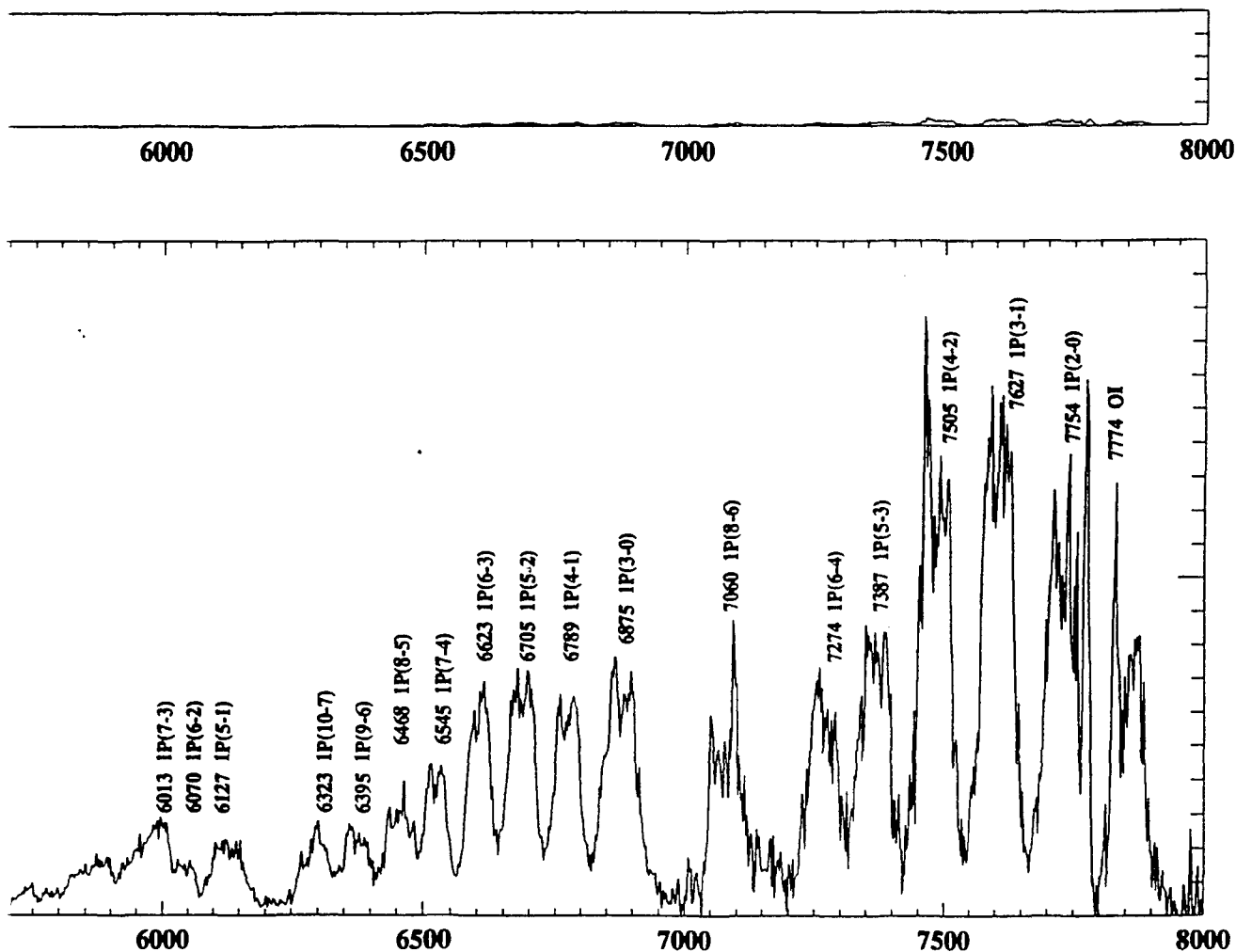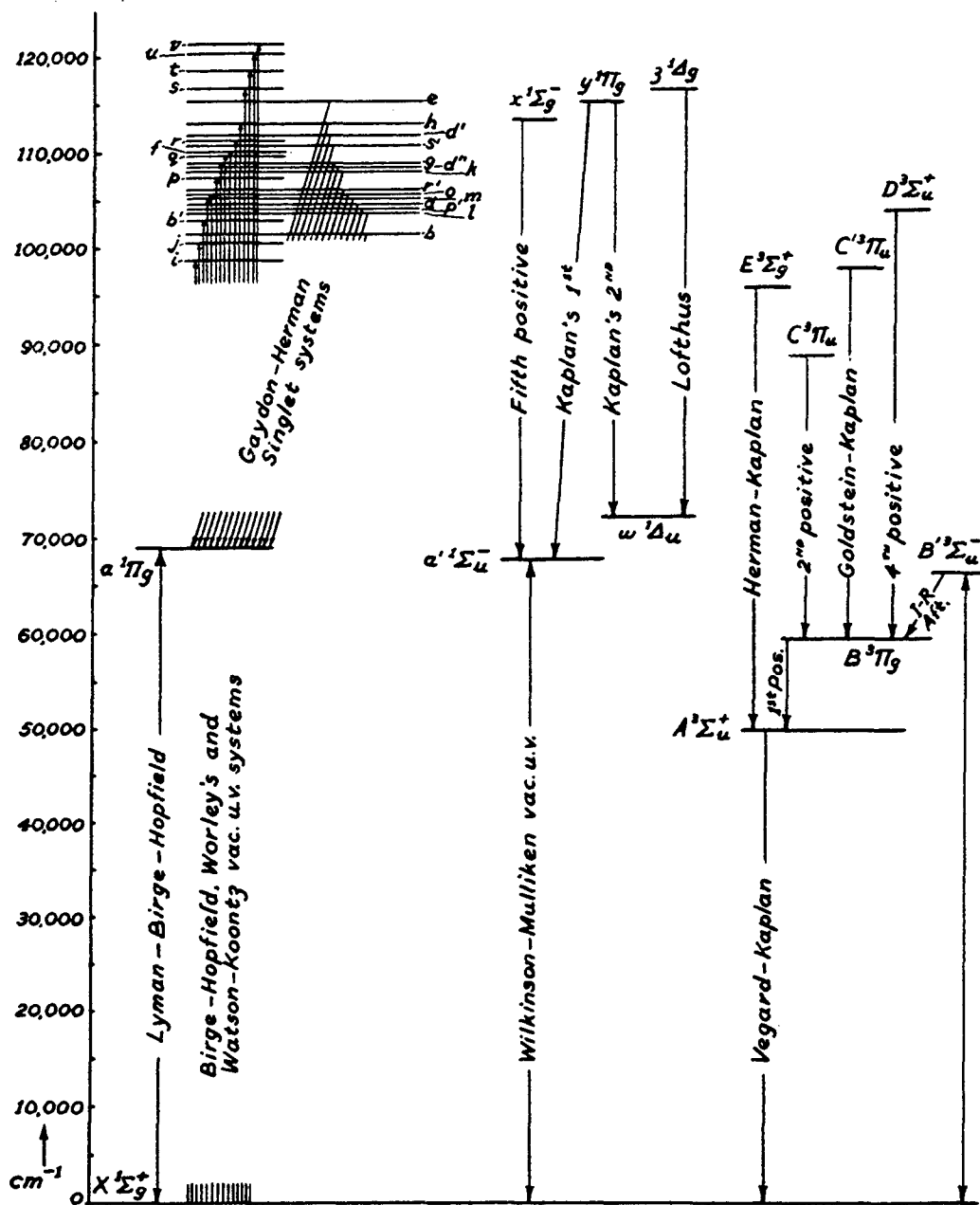# EXCEDE III VISIBLE SCAN No. 10 at 157.4 Sec. and 108.3 Km.

4500   5000   5500   6000   6500   7000

.h (A)

Wavelength (A)

Figure 7b: Optical Spectrum at 108.3 km From the EXCEDE III Experiment.

157.4 Sec. and 108.3 Km.

Labeled spectral peaks (bottom plot):
6013 1P(7-3), 6070 1P(6-2), 6127 1P(5-1), 6323 1P(10-7), 6395 1P(9-6), 6468 1P(8-5), 6545 1P(7-4), 6623 1P(6-3), 6705 1P(5-2), 6789 1P(4-1), 6875 1P(3-0), 7060 1P(8-6), 7274 1P(6-4), 7387 1P(5-3), 7505 1P(4-2), 7627 1P(3-1), 7754 1P(2-0), 7774 OI

x-axis: 6000, 6500, 7000, 7500, 8000

ɔm the EXCEDE III Experiment.

③

Figure 8: Energy Level Diagram for N$_2$.

25

Kaplan ground state bands are denoted, however, very little strength is apparent in these spectra. These emissions are forbidden transitions and therefore are not prompt.

A few of the strongest $NO\gamma$ bands located in the UV are also denoted on the figure and appear to be weak. Two of these $NO\gamma$ bands are located at 2262 and 2479 Å where well defined peaks exist. However, these peaks are better identified with the Herman-Kaplan 0-4 band at 2471 Å and the $N_2(4P)$ 0-0 band at 2261 Å. This is because very little strength in other $NO\gamma$ emissions is seen (e.g. $NO\gamma$ 0-1 at 2370 Å or $NO\gamma$ 0-2 at 2596 Å) whereas many other Herman-Kaplan and $N_2(4P)$ series of bands are clearly identified in the data.

The $N_2(1P)$ bands and the $N_2^+(1N)$ bands make up the majority of the spectrum between 3000 and 5000 Å. The $N_2^+(1N)$ 0-0 band at 3914 Å is the largest intensity emission in the spectrum. Other prominent bands are the $N_2^+(1N)$ 0-1 band at 4278 Å, and the $N_2(2P)$ 0-0 and 0-1 emissions at 3371 and 3577 Å, respectively. The $N_2(1P)$ series of bands are the prominent features from 6000 to 8000 Å and appear to have larger FWHM when plotted against λ.

Several atomic lines have also been identified, the most intense being the 5577 Å OI line. This is a delayed emission feature and is responsible for the characteristic green color seen in natural aurora; another detected oxygen line is at 7774 Å. Other atomic lines easily identified are due to atomic nitrogen at 3466 Å $N(^2P)$ and 5005 Å NII.

Plates 3 and 4 are spectrograms of all unattenuated UV and Visible spectral scans obtained, respectively. The scans have been normalized by their associated boresight photometer data sets on a sample by sample basis. This normalization is important for removing any temporal perturbations in the electron beam such as the beam power oscillations caused by the Attitude Control System.

While the UV data scans have negligible non-source background the Visible spectral scans have significant background which must be subtracted off before dividing by the boresight photometer data. The background was determined by examining the beam-off spectra and was found to be the same each scan.

The spectral scans from the Visible spectrometer all have arbitrary units and were normalized to the $N_2^+(1N)$ 0-1 emission at 4278 Å. The 4278 Å band was used for normalizing the other spectral features because of the quality of its measurement and because it is easily related to the $N_2^+(1N)$ 0-0 band at 3914 Å. The area under the 4278 Å emission band was

defined to be equal to one; for scans where this line was not available, a normalization constant was derived by interpolating between spectra.

The UV spectral scans are also plotted in relative intensity units and have been normalized using the $N_2(2P)$ 1-0 band at 3157 Å, a region where the UV and Visible spectra overlap. The area under this emission band in the UV spectra was scaled to match the same emission found in the Visible spectrometer data set; this in turn references all spectra to the 4278 Å emission.

The Visible spectrum reveals numerous strong emission bands. The prompt N_2 1N and 2P series characterize the spectrum below 5000 Å. The $N_2(1P)$ series is observed starting at ~6000 Å; although the peak intensities are considerably less than the emissions below 5000 Å, each band is significantly broader in wavelength. The other prominent emission throughout the flight is the 5577 Å delayed emission from atomic oxygen.

The tendency for spectral features to appear broadened at longer wavelengths is largely a consequence of the spectrometer design. The spectral scans are all measured as a function of wavelength because the spectral grating in the spectrometer is rotated in steps of constant λ. The expression relating changes in $\Delta\nu$ to $\Delta\lambda$ is given by $\Delta\nu = -\Delta\lambda/\lambda^2$. Therefore, two peaks with the same $\Delta\nu$, but having wavelengths differing by a factor of two, will appear to have line widths differing by a factor of 4 when plotted as a function of wavelength.

The strongest band in every scan is the $N_2^+(1N)$ 0-0 band at 3914 Å. The count rates from this emission were sufficiently high in the unattenuated spectral scans to drive the photomultiplier tube into saturation, with the possible exception of times near apogee. Unfortunately, a recent failure of the detector in the laboratory precluded any post flight nonlinearity calibration to further examine the behavior of the tube near saturation. Therefore, we must rely exclusively on the attenuated scans for measurements of the 3914 Å emission band.

Normalizing all spectra to the 4278 Å emission allows the comparison of band efficiencies over the entire flight. All prompt emission bands in the UV and visible spectrum appear to be approximately constant in intensity over all respective spectral scans implying that the emission rate is at least approximately independent of altitude. A slight reduction in intensity is observed for the delayed 5577 Å line over the flight; however, the interpretation of this feature requires further consideration of the geometry and oxygen concentrations.

27

5.7 *Attenuated Spectra.* Plate 5 shows a condensed plot of the attenuated scans from the Visible spectrometer after background subtraction and normalization. Although the data are noisy, spectral emission features are seen at 3914 and 4278 Å. We note that the measurements of the 3914 Å emission in these spectral scans do not approach saturation.

The absolute intensities of the 4278 Å band measured from the attenuated and unattenuated scans have been compared and are in excellent agreement.

Figure 9 is a plot of the ratio of the N_2^+(1N) 0-0 band intensity at 3914 Å to the N_2^+(1N) 0-1 band intensity at 4278 Å over the flight using the attenuated spectral scans. The ratios derived from data having scan numbers between 20 and 40 correspond to altitudes above ~110 km. The counting statistics for these scans (particularly the 4278 Å emissions) are very poor and are reflected in the large error bars. Given the large uncertainties, the ratio is consistent with being a constant throughout the times shown in Figure 9.

The two band emissions result from the same initial molecular states but different final states and are related to each other by their respective Einstein radiative coefficients if quenching or branching is not significant. A ratio of 3.27 is obtained [*Jones*, 1974] based on the work of *Shemansky and Broadfoot* [1971]; The EXCEDE III data are consistent with a constant value of ~2.7 over the altitude range (85-115 km) of the flight.

5.8 *Comparison of Artificial and Natural Aurora.* Figures 10a-c are plots of UV and optical spectra compiled by *Jones*, [1974] typical of IBC 2-3 natural aurora at altitudes between 110 and 120 km. The fundamental difference between the EXCEDE III spectra obtained and that from a natural aurora is the absence of delayed emissions in the EXCEDE III spectra. The difference in the temporal history of the emissions seen in the EXCEDE III data results from the significantly shorter dosing times inherent in the design of the EXCEDE III experiment. Long lived emissions such as the 6300 Å OII emission (Figure 10c) and the N_2 Vegard-Kaplan emissions between 2100 and 3400 Å (Figure 10a) are clearly seen in natural aurora but are absent from the EXCEDE III spectral scans. A comparison of prompt emissions indicate that the two data sets have very similar prompt spectral features.
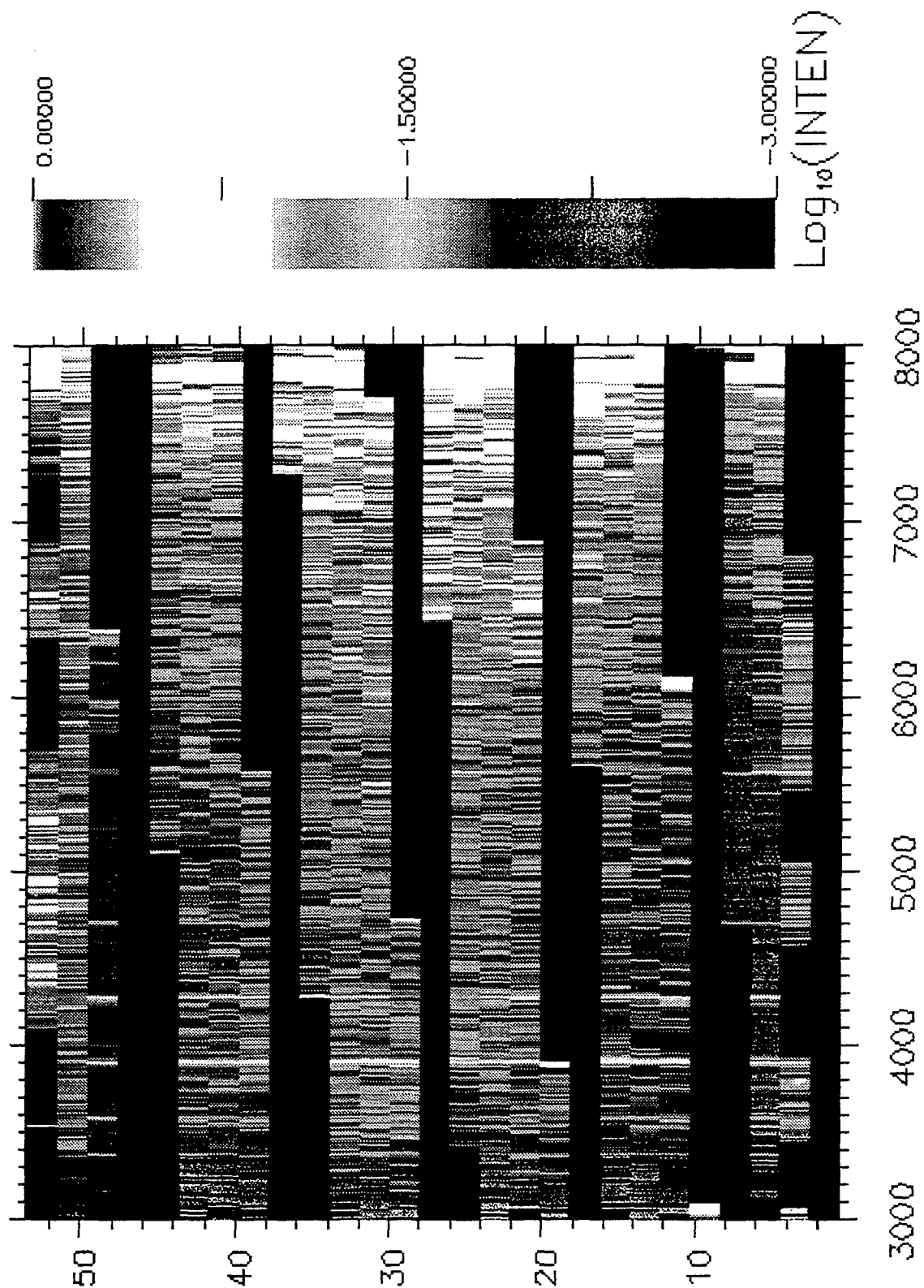
EXCEDE III Attenuated Visible Spectra

Plate 5: Visible Spectrometer Spectral Scans with Neutral Density Filter.
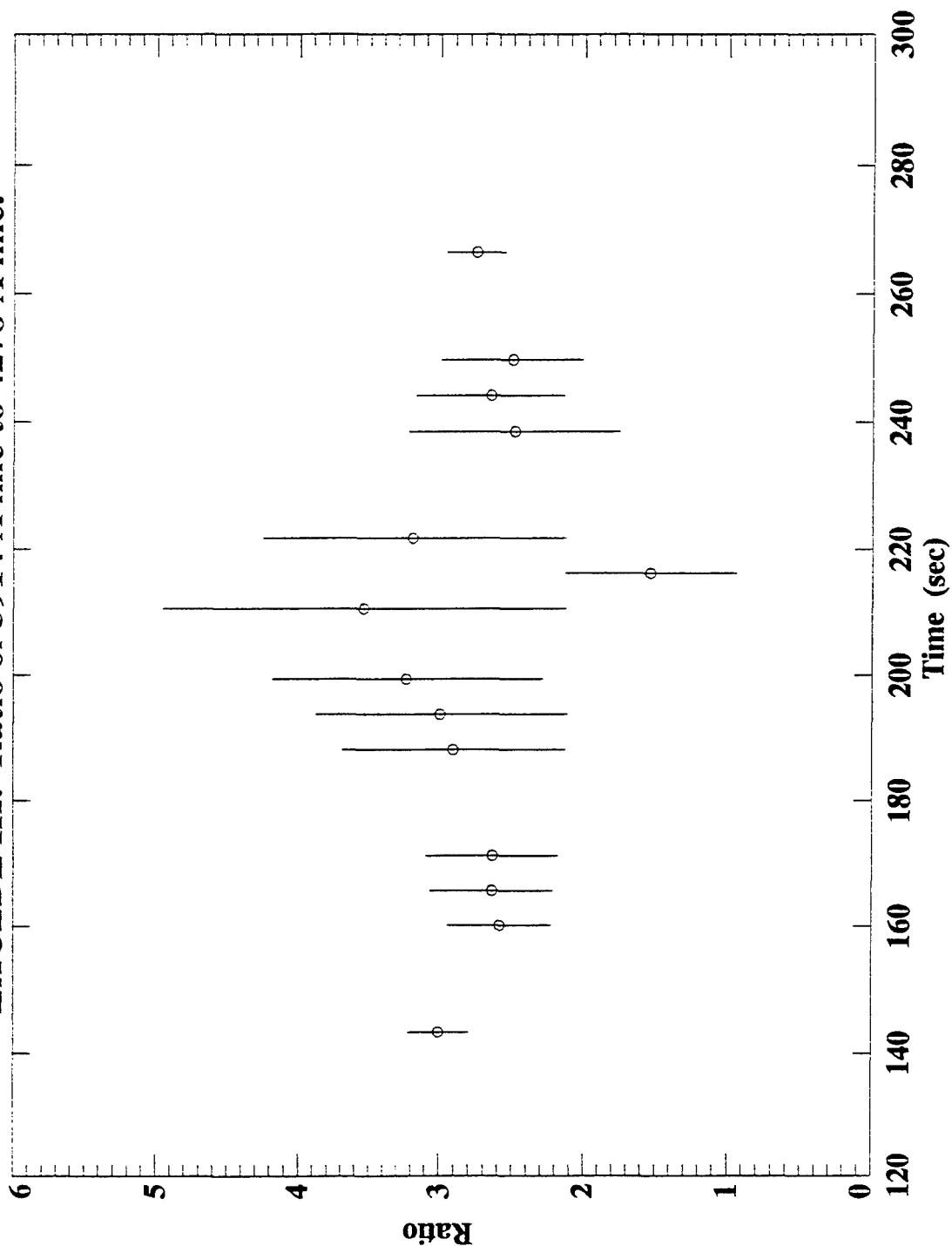
EXCEDE III: Ratio of 3914 A line to 4278 A line.

Figure 9: Ratio of $N_2^+(1N)$ 0-0 (3914 Å) to 0-1 (4278 Å) Bands for the Attenuated Spectral Scans.
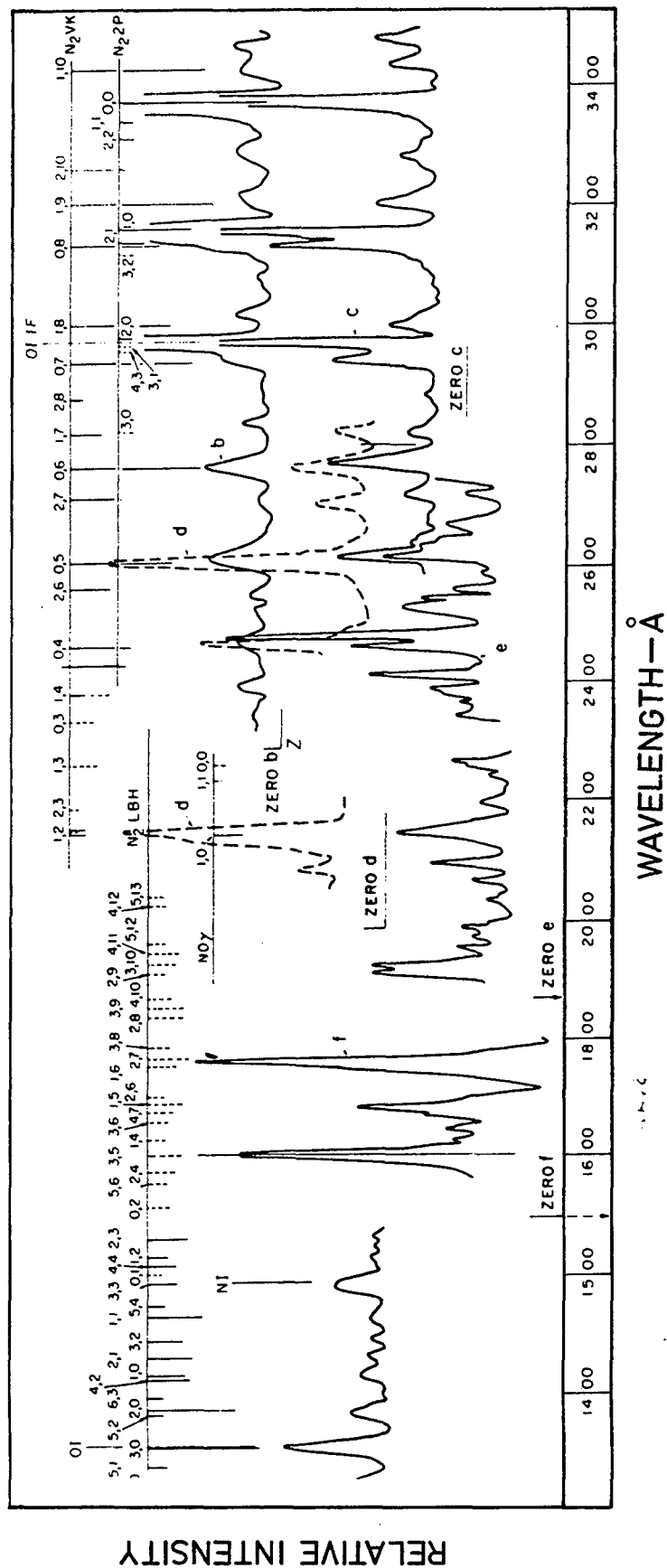
Figure 10a: UV Spectra (1300 to 3500 Å) From an IBC II-III Natural Aurora Occurring Between 110 and 120 km [*Jones*, 1974].
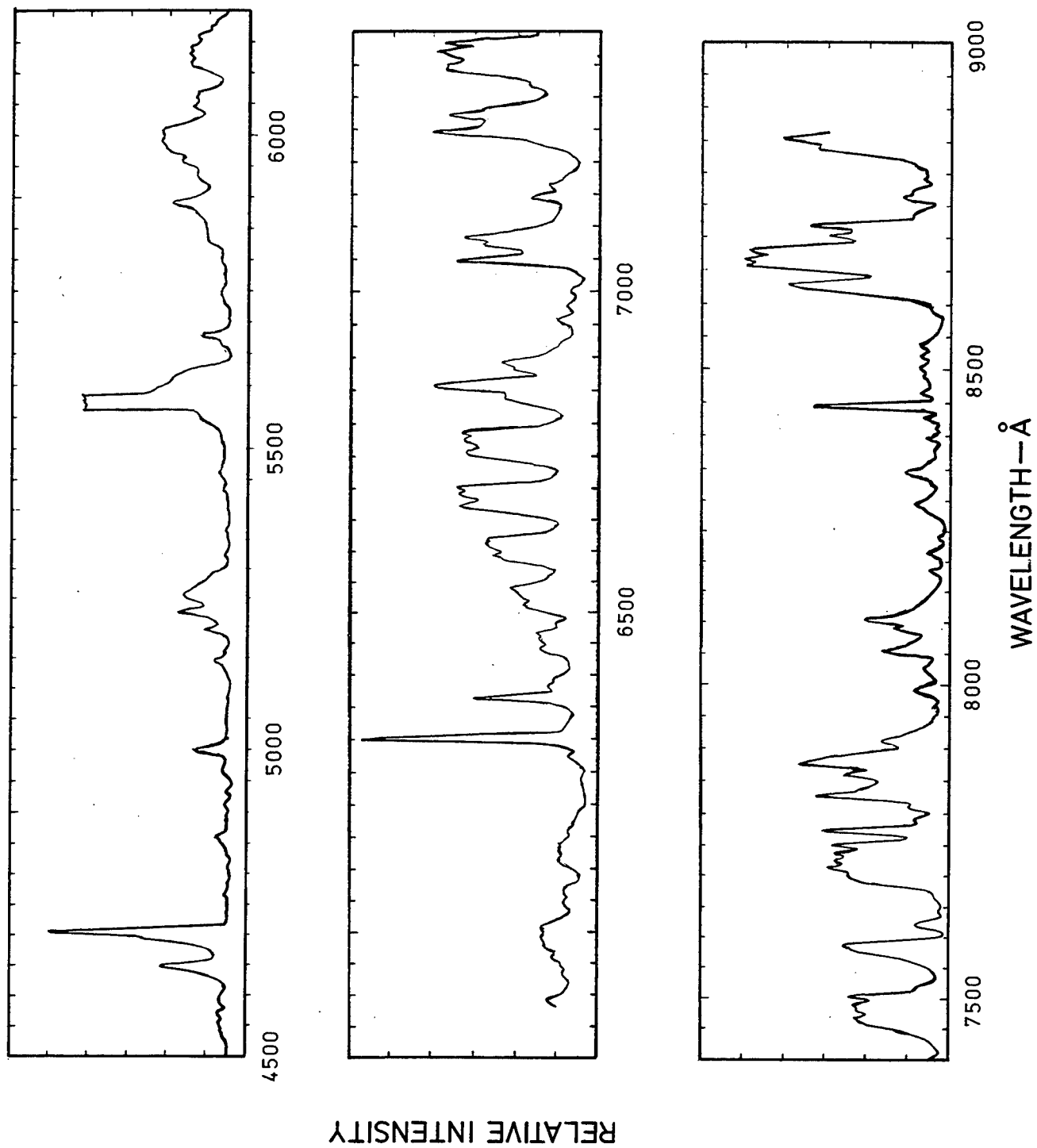
Figure 10b: Optical Spectra (3100 to 4700 Å) From an IBC II-III Natural Aurora Occurring Between 110 and 120 km [*Jones*, 1974].
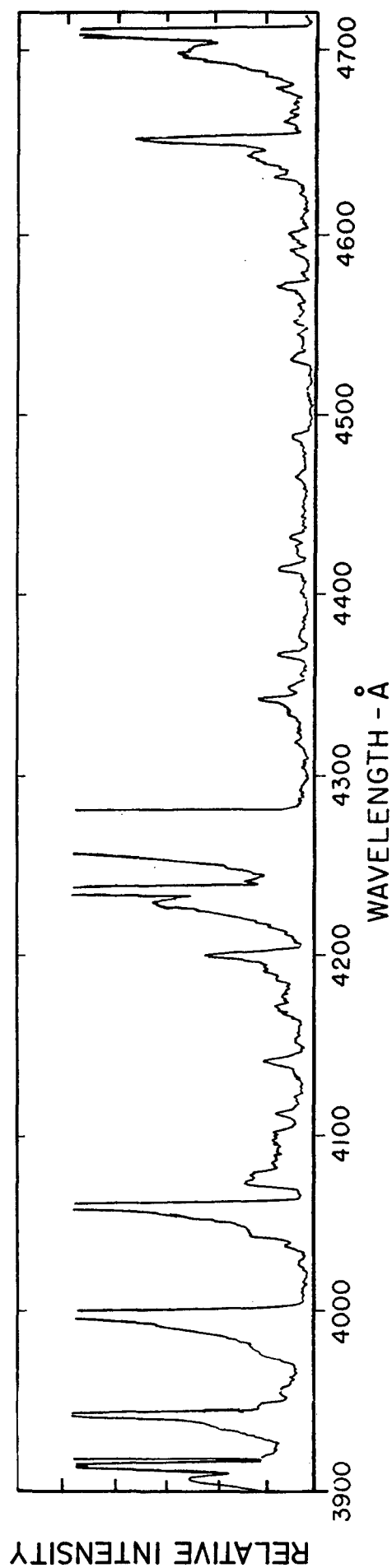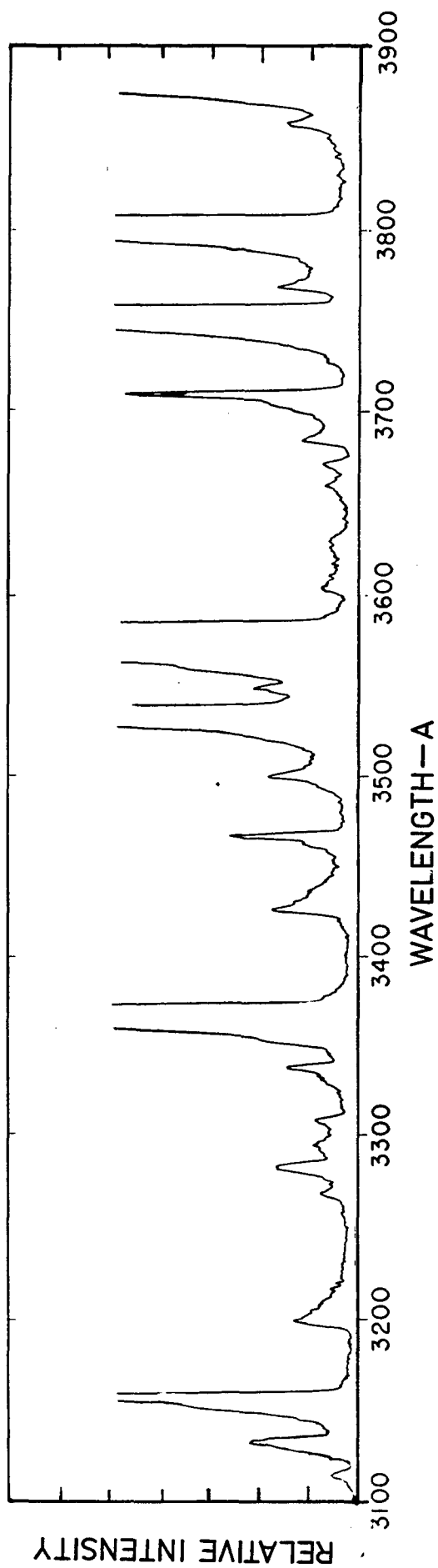
Figure 10c: Optical Spectra (4500 to 9000 Å) From an IBC II-III Natural Aurora Occurring Between 110 and 120 km [Jones, 1974].

33

5.9 *Spectral Efficiencies.* As was discussed above, all spectral scans have been normalized to the $N_2^+(1N)$ 0-1 band intensity at 4278 Å which was set equal to one. The band intensity is the area under the molecular emission or $\Sigma I_j \delta\lambda$, where I_j is the intensity in the *jth* bin of the transition of interest and $\delta\lambda$ is the width of the I_j bin.

The denominator (i.e. the 4278 Å band intensity) has already been set equal to one, therefore, the efficiency of a particular emission is equal to the area underneath the band after any continuum has been removed. Figures 11 and 12 are compilations of this ratio for numerous wavelength regions. No attempt to fit individual peaks has been made.

The efficiencies derived from the Visible spectrometer data set $(\lambda > 3000$ Å) are consistent with constant values over the entire flight. This implies that the relative production rates of these prompt emissions are independent of altitude.

The efficiencies for the UV spectrometer data set with the exception of the $N_2(2P)$ emissions near 3000 Å are not constant over the flight. All emissions below ~ 2900 Å indicate enhancements at 170 s and after 210 s. These changes can be observed by comparing the yields at shorter wavelengths to the 3159 Å emission (which is roughly constant) for the two spectra at 157.4 s and 228.4 s (see Appendix A).

The $N_2^-(1N)$ 0-0 band at 3914 Å would make a better reference for determining efficiencies than the $N_2^+(1N)$ 0-1 band because of its prominence in aurora and its use as a measure of the primary ionization and, hence, the energy deposition in the atmosphere. However, a better experimental measure of the 0-1 band at 4278 Å was obtained and it is therefore used in place in the 3914 Å band. The ratios can be related to the 3914 Å band by dividing by ~ 2.7, the ratio of 3914 Å to 4278 Å band intensities derived from the attenuated scans discussed above.

5.10 *3805/3914 Ratio.* Emissions at 3805 Å result from the excitation of the (0,2) second positive band of N_2 denoted $N_2(2P)$ 0-2 [*Borst and Imami*, 1973; *Burns et al.*, 1969]. The excited state produced by electron impact is $C^3 \Pi_u$ which has a lifetime of 50 ns [*Jones*, 1974] and decays to $B^3 \Pi_g$. The excitation functions for the $N_2(2P)$ v' = 0, v" transition (=2 in this case) are typified by the (0,0) transition [*Jobe et al.*, 1967]. The cross section threshold is ~ 11
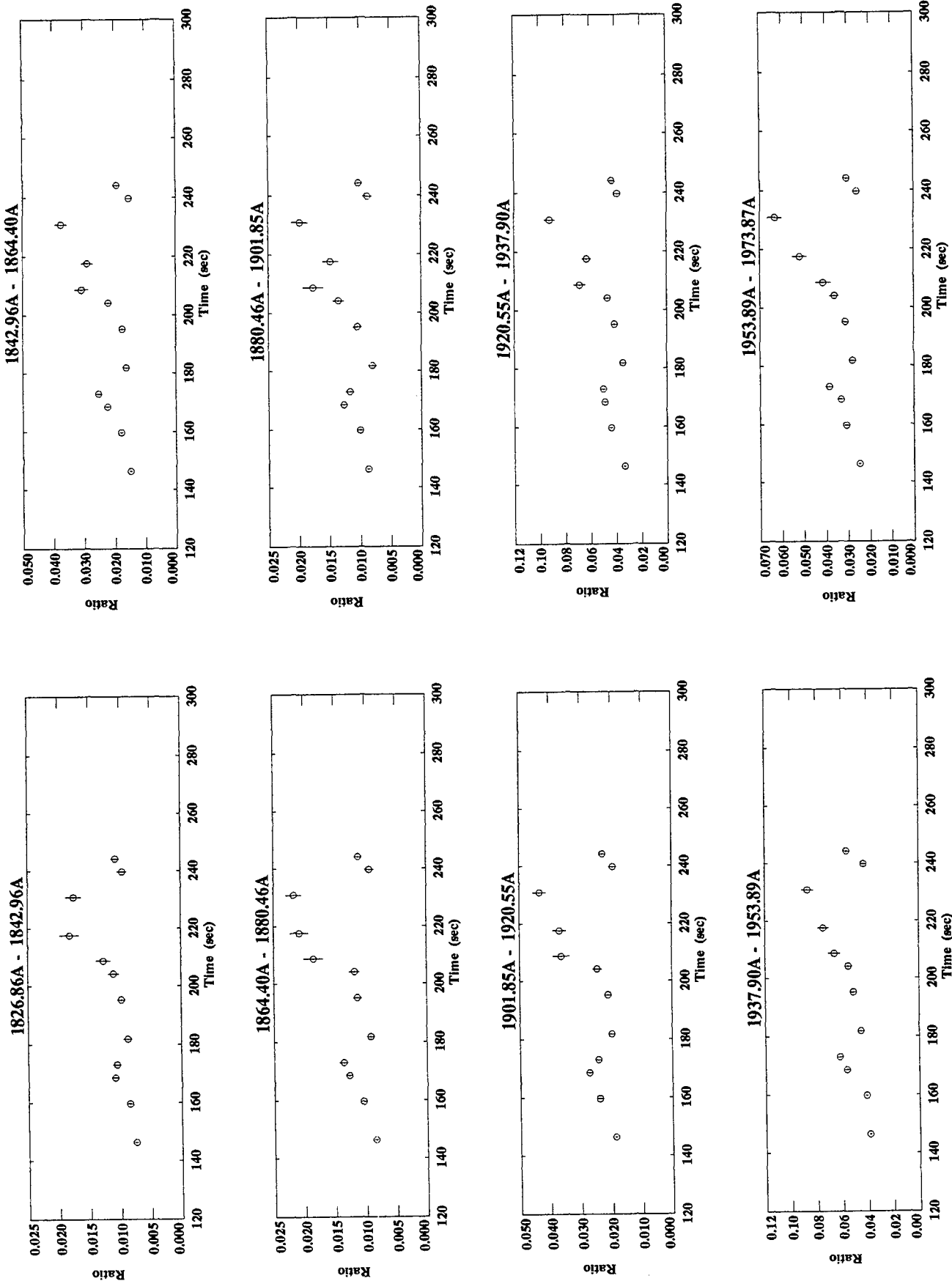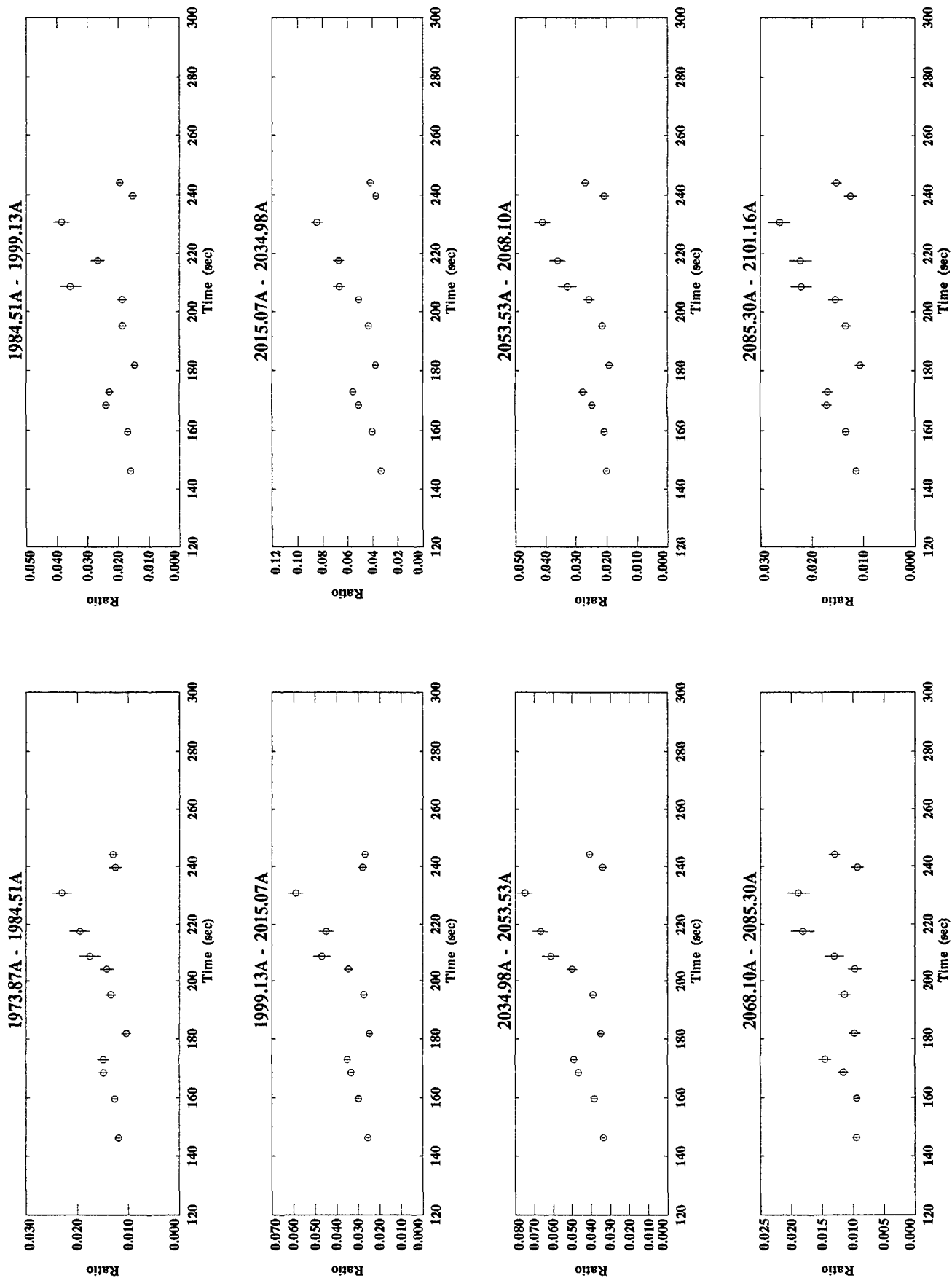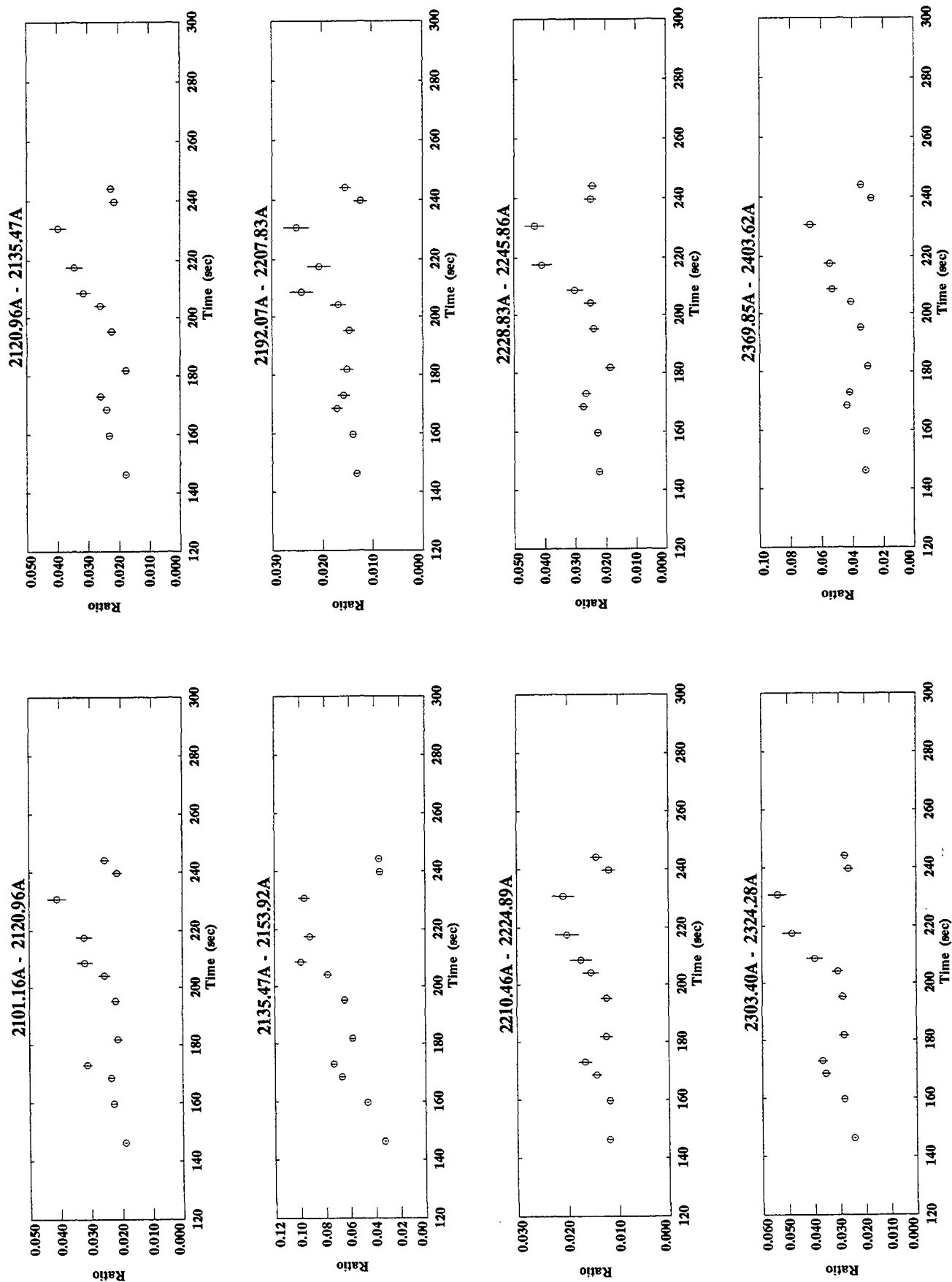
Figure 11: UV Spectral Efficiencies With Respect to the N_2^+(1N) 0-1 Band at 4278 Å.

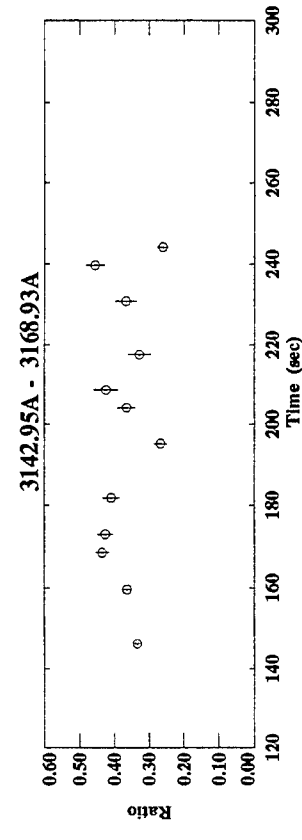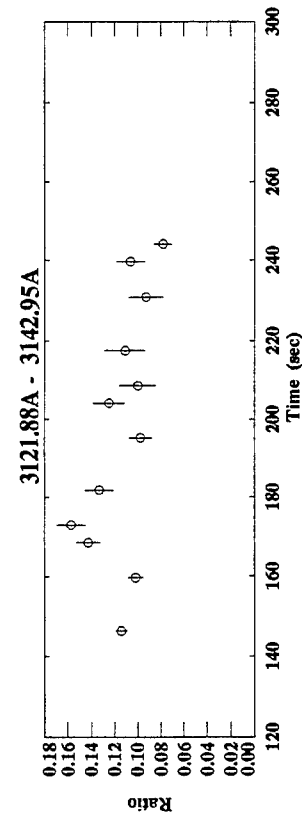Figure 11: UV Spectral Efficiencies With Respect to the N_2^+(1N) 0-1 Band at 4278 Å.
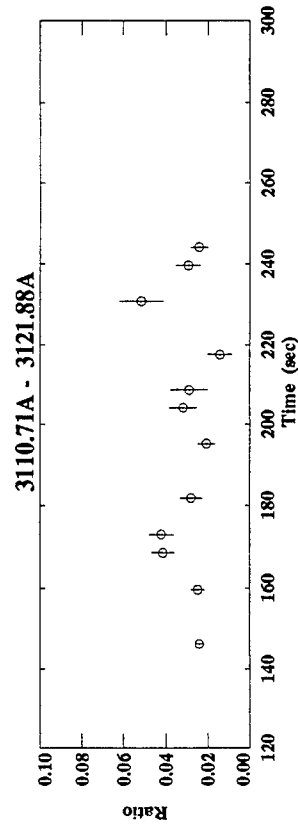
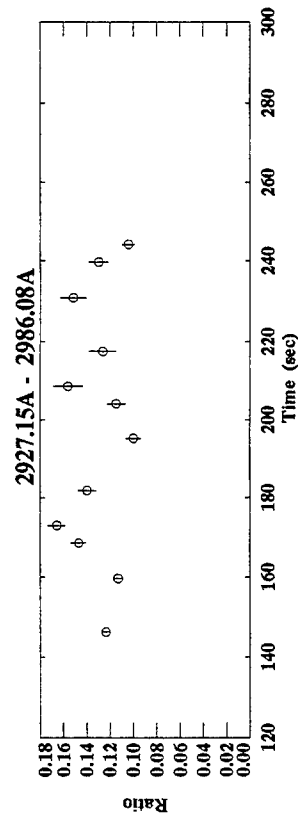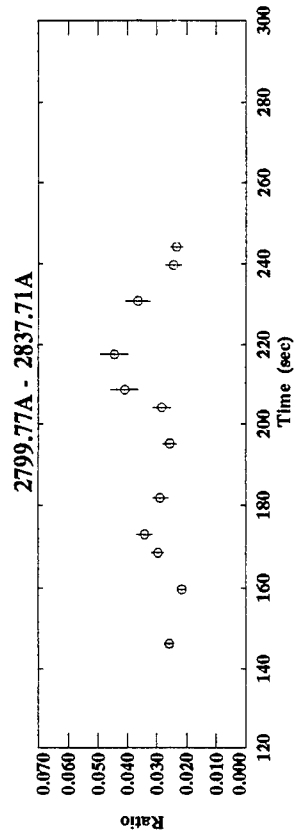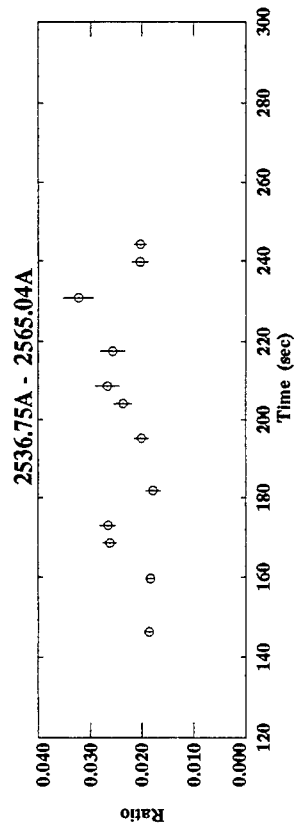Figure 11: UV Spectral Efficiencies With Respect to the N_2^+(1N) 0-1 Band at 4278 Å.
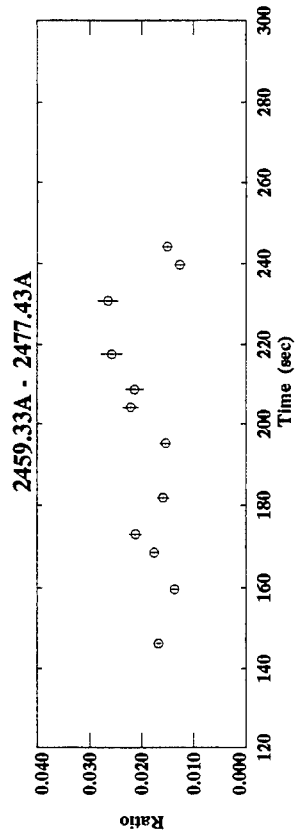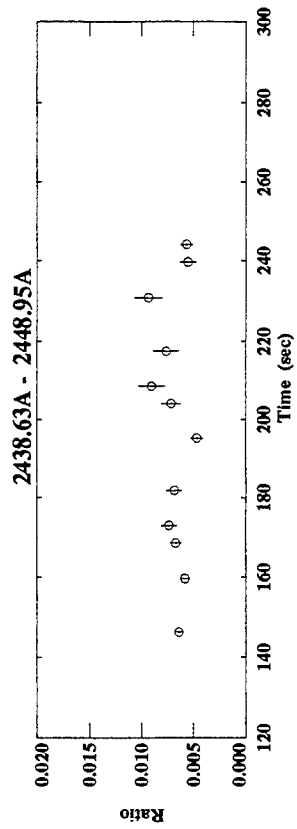
Figure 11: UV Spectral Efficiencies With Respect to the N_2^+(1N) 0-1 Band at 4278 Å.
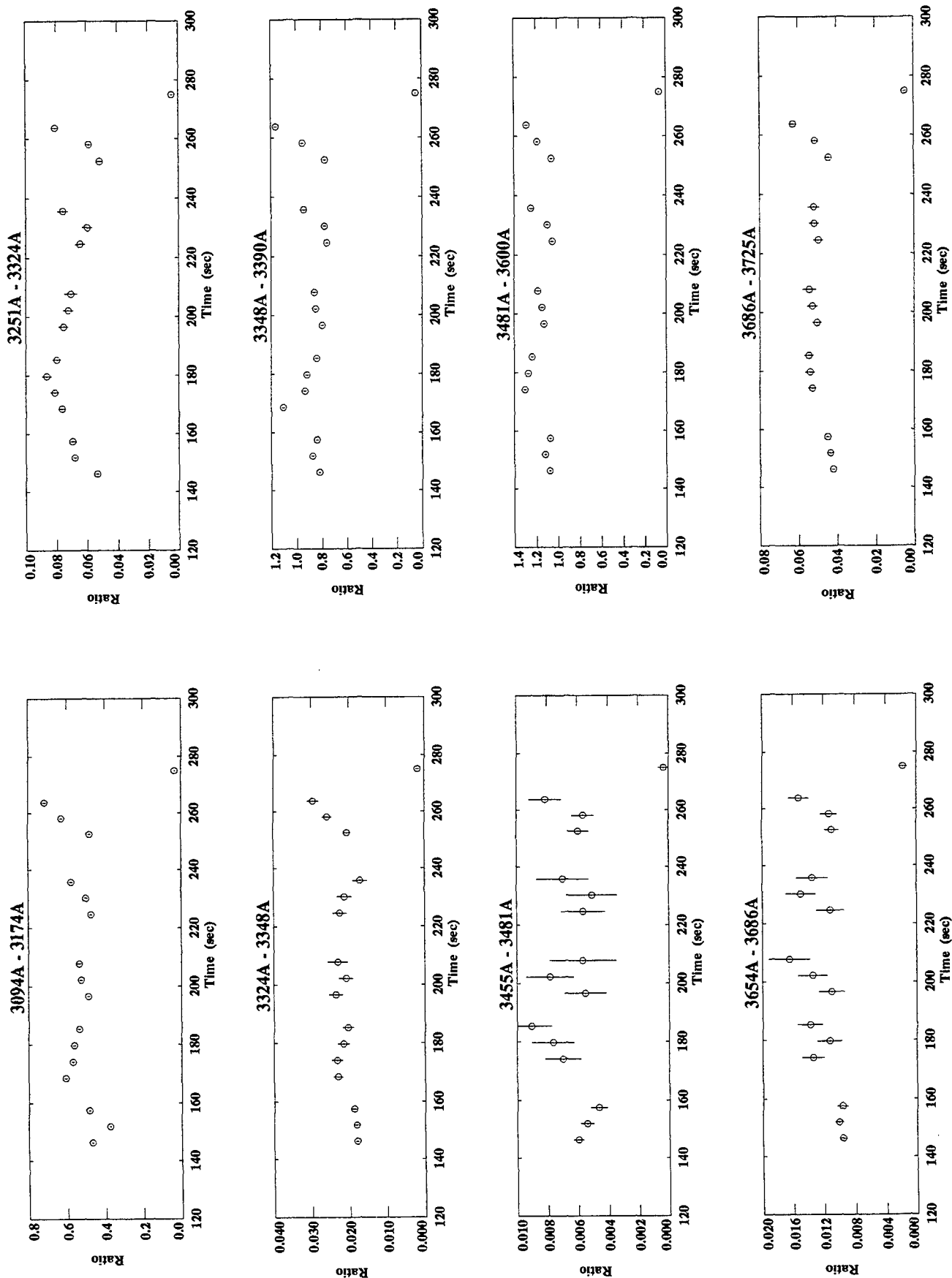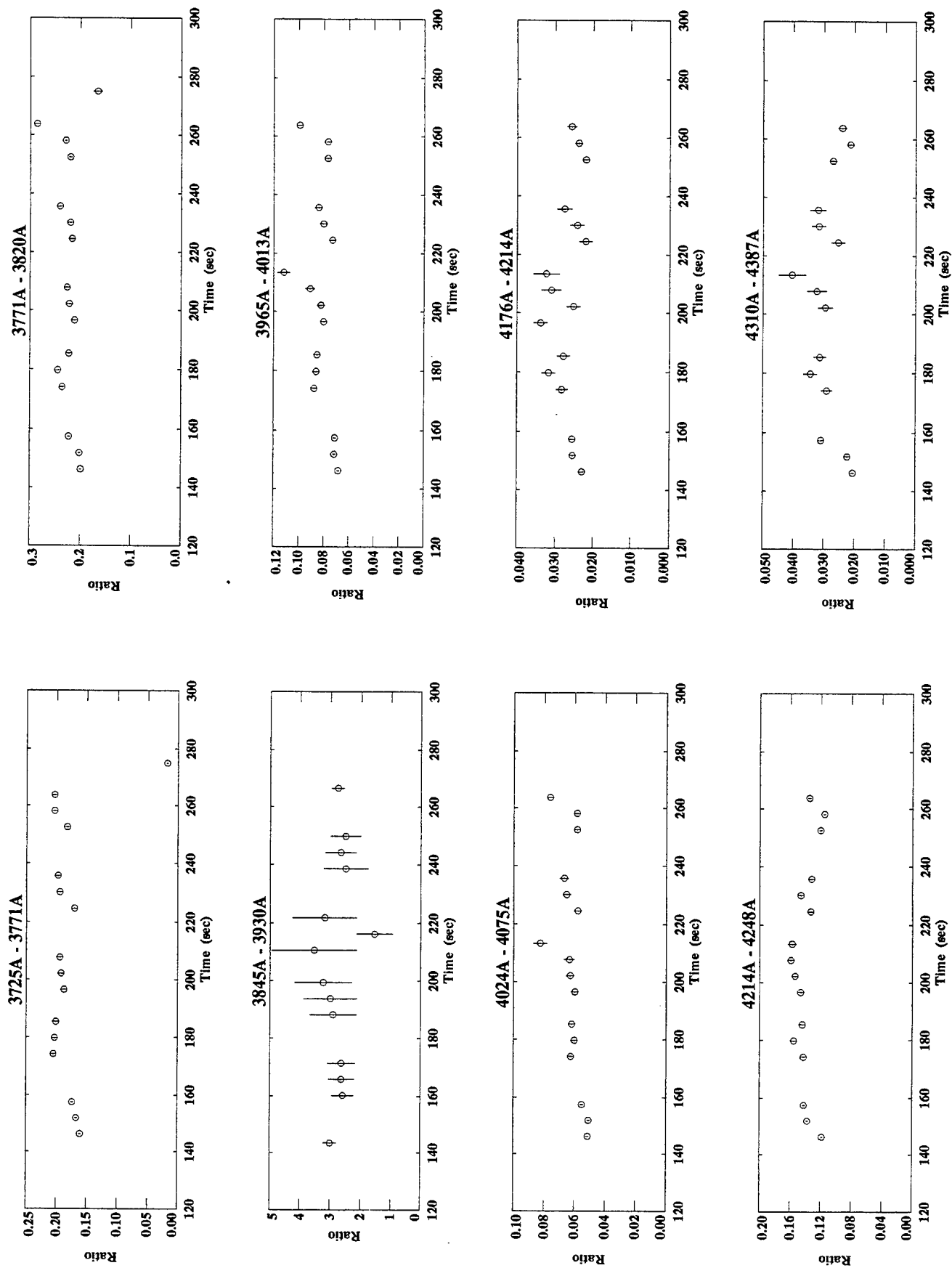
38

Figure 12: Optical Spectral Efficiencies With Respect to the $N_2^+(1N)$ 0-1 Band at 4278 Å.

Figure 12: Optical Spectral Efficiencies With Respect to the N_2^+ (1N) 0-1 Band at 4278 Å.
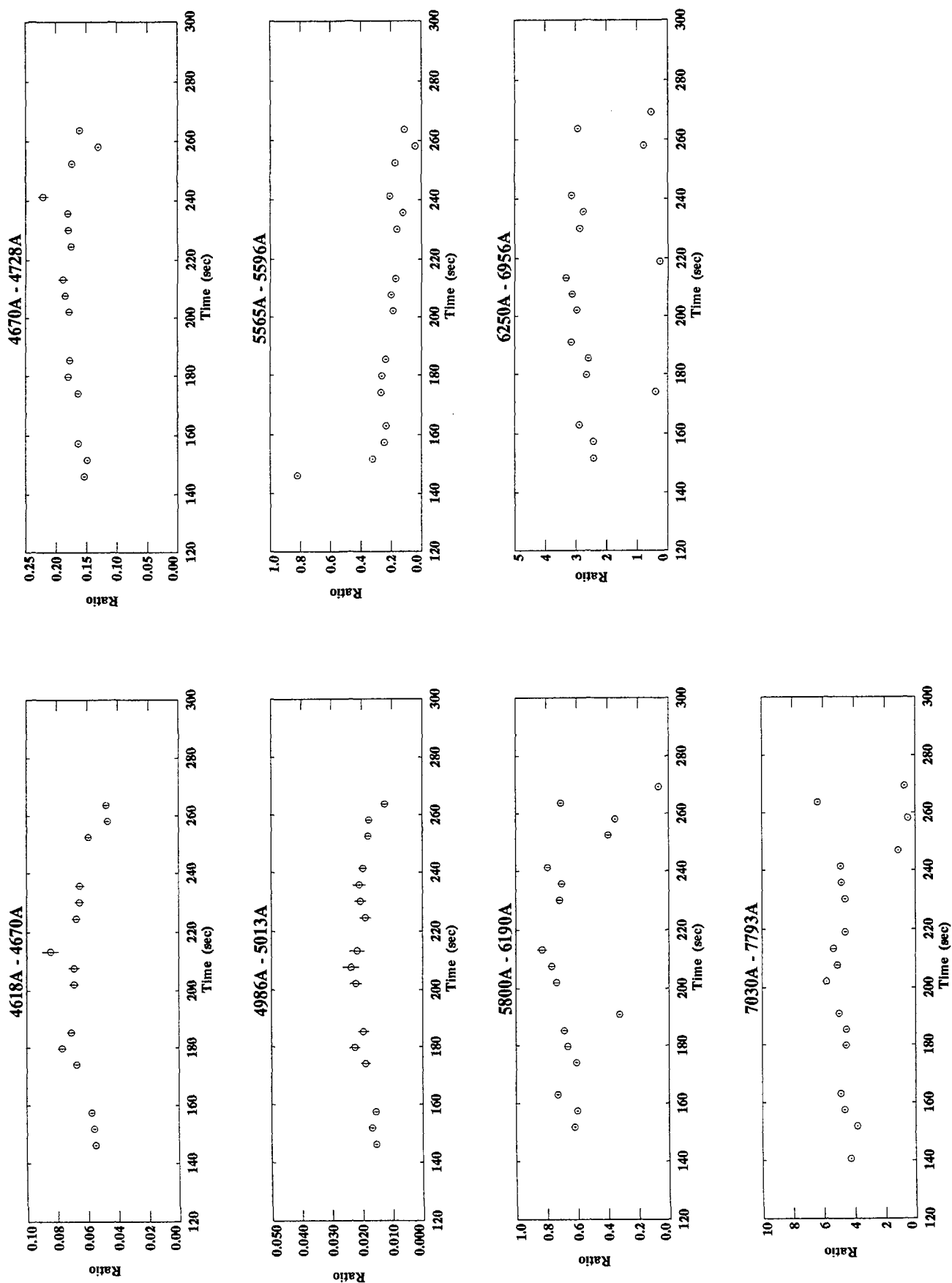
Figure 12: Optical Spectral Efficiencies With Respect to the N_2^+(1N) 0-1 Band at 4278 Å.

eV with a sharp resonance peak near 14 eV and subsequent rapid decrease with energy [*Burns et al.*, 1969]; hence, emissions at 3805 Å are a diagnostic for the low-energy secondary electrons produced by the primary beam electrons [*Borst and Imami*, 1973].

A value for the ratio of the 3805 Å to 3914 Å emission was obtained from the optical spectrometer data. The ratio of the band intensity in the spectral region 3771 to 3820 Å containing the 3805 Å emission to the 4278 Å band was divided by the 3914/4278 Å ratio obtained from the attenuated optical spectral scans and is plotted in Figure 13. A value of ■0.085 is obtained which is in excellent agreement with the value of 1/12 found in natural aurora [*Jones*, 1971].

6. Summary

A goal of the EXCEDE III atmospheric energy deposition experiment was to monitor the spectral excitations from the energy deposition profile produced by the ~18 Ampere ~2.5 keV electron beam. Two Ebert-Fastie spectrometers were used to collect UV and optical spectra between the altitudes 82 and 115 km and over the spectral range 1800 to 8000 Å. Spectral features have been identified and efficiencies relative to the N_2^+(1N) 0-1 band at 4278 Å have been calculated. The measured spectra were compared with those obtained from natural aurora and appear to differ primarily by the absence of delayed transitions. Finally, all spectra have been presented and a data base has been prepared.
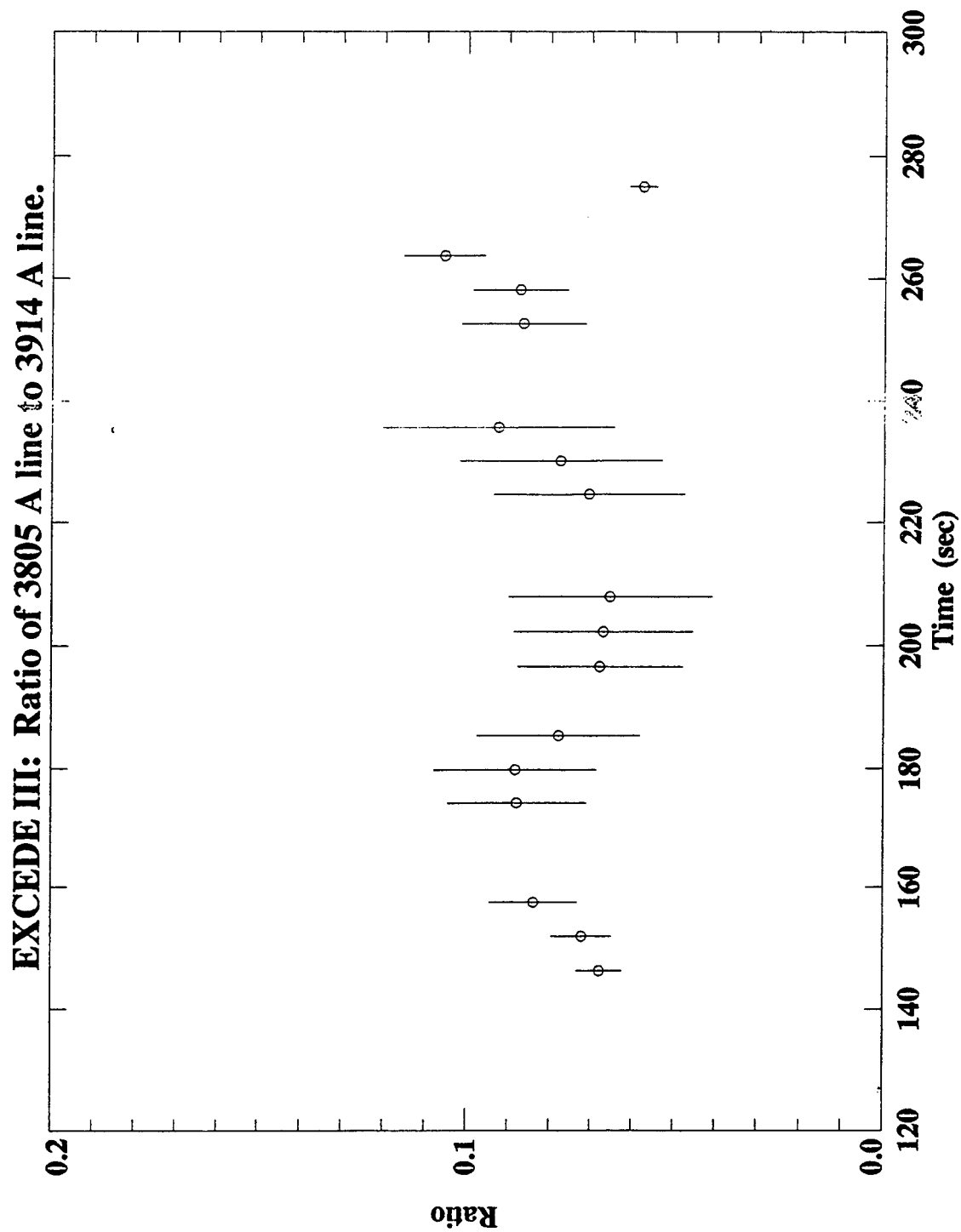
EXCEDE III: Ratio of 3805 A line to 3914 A line.

Figure 13: Ratio of the $N_2(2P)$ 0-2 Band at 3805 Å to $N_2^+(1N)$ 0-0 at 3914 Å.

References

1. Borst, W.L., and M. Imami, "Production of secondary electrons in nitrogen by fast electrons and simultaneous excitation of N_2 bands," J. Appl. Phys., **44**, 1133-1141 (1973).

2. Burns, D.J., F.R. Simpson, and J.W. McConkey, "Absolute cross sections for electron excitation of the second positive bands of nitrogen," J. Phys. B, **2**, 52-64 (1969).

3. Chamberlain, J.W., Physics of the Aurora and Airglow, (Academic Press, New York, 1961).

4. Ebert, H., Wied. Ann, **38**, 489 (1889).

5. Fastie, W.G., J. Opt. Soc. Am., **42**, 641 (1952).

6. Fastie, W.G., J. Opt. Soc. Am., **42**, 647 (1952).

7. Jobe, J.D., F.A. Sharpton, and R.M. St. John, "Apparent cross sections of N_2 for electron excitation of the second positive system," J. Opt. Soc. Am., **57**, 106-107 (1967).

8. Jones, A.V., Aurora, D. Reidel Pub. Co., Dordrecht, Holland, 1974.

9. Lee, E.T.P., F. Bien, M. Zahniser, R. Lyons, C. Kolb, and R.R. O'Neil, Private Communications.

10. O'Neil, R.R., F. Bien, D. Burt, J.A. Sandock, and A.T. Stair, Jr., "Summarized results of the artificial auroral experiment, Precede," J. Geophys. Res., **83**, 3273-3280 (1978).

11. O'Neil, R.R., O. Shepherd, W.P. Reidy, J.W. Carpenter, T.N. Davis, D. Newell, J.C. Ulwick, and A.T. Stair, Jr., "EXCEDE 2 Test, an Artificial Auroral Experiment: Ground-Based Optical Measurements," J. Geophys. Res., **83**, No. A7, 3281-3288 (1978).

12. O'Neil, R.R., A.T. Stair, Jr., W.R. Pendelton, Jr., and D. Burt, "The EXCEDE SPECTRAL Artificial Auroral Experiment: An Overview," in Artificial Particle Beams in Space Plasma Studies," edited by B. Grandal, (Plenum, New York, 1982), pp. 207-215.

13. Pearse, R.W.B. and A.G. Gaydon, The Identification of Molecular Spectra, Halston Press, London, 1976, p. 218.

14. Rappaport, S.A., R.J. Rieder, W.P. Reidy, R.L. McNutt, Jr., J.J. Atkinson, and D.E. Paulsen, "Remote X-Ray Measurements of the Electron Beam from the EXCEDE III Experiment," J. Geophys. Res., (accepted for publication, 1993).

15. Rieder, R.J., T. Keneshea, R.L. McNutt, Jr., S.A. Rappaport, D.E. Paulsen,"Characterization of the Energy Deposition Produced by the Primary Electron Beam on the EXCEDE III Program," VI-2067, Visidyne Inc., Burlington, MA (1993).

16. Samson, J.A., <u>Vacuum Ultraviolet Spectroscopy</u>, John Wiley and Sons, New York, 1967, p. 54.

17. Shemansky, D.E. and Broadfoot, A.L., J. Quant. Spectrosc. Radiat. Transfer, **11**, 1401, (1971)